UCRL 2932
UNCLASSIFIED

# UNIVERSITY OF CALIFORNIA

# Radiation Laboratory

## CHEMISTRY DIVISION QUARTERLY REPORT

December 1954, January, February 1955

BERKELEY, CALIFORNIA

## DISCLAIMER

UCRL-2932
Unclassified Chemistry

UNIVERSITY OF CALIFORNIA
Radiation Laboratory
Berkeley, California

Contract No. W-7405-eng-48

# CHEMISTRY DIVISION QUARTERLY REPORT

December 1954, January, February 1955

March 30, 1955

Printed for the U. S. Atomic Energy Commission

# CHEMISTRY DIVISION QUARTERLY REPORT

December 1954, January, February 1955

Contents



*Previous Quarterly Reports: UCRL-2841, UCRL-2709

UCRL-2932
Unclassified Chemistry

# CHEMISTRY DIVISION QUARTERLY REPORT

December 1954, January, February 1955

Radiation Laboratory, Department of Physics
University of California, Berkeley, California

March 30, 1955

## BIO-ORGANIC CHEMISTRY

M. Calvin, Director

Edited by B. M. Tolbert

## RESPIRATORY CARBON-14 PATTERNS IN HUMANS

B. M. Tolbert, Martha R. Kirk, and John H. Lawrence

Carbon-14, the most useful radioactive isotope of carbon, has been extremely important in chemical and biochemical research for the last ten years. It is difficult to detect and measure the radioactivity from this weak beta emitter, and in animal experiments it is not possible to detect the radioactivity or its location from outside the body. Thus animal studies using this isotope usually require sacrifice of the animal. Because of this difficulty, carbon-14 has not yet become a useful tool in clinical medicine.

While the carbon-14 cannot be detected in animals in situ, it can be measured as it is excreted. Of the various excretion routes for carbon in the body, the breath carbon dioxide is the most important in terms of quantity, and responds rapidly to changes in metabolic level of the body. The breath excretion of carbon-14 following administration of a labeled organic compound can therefore be used to study the metabolism of this specific compound and of the given labeled carbon atom in the compound. Furthermore, if one knows the respiratory pattern of a given labeled compound in an animal system, variations in this pattern can be interpreted in terms of the physiological state of the animal on the biochemical level.

The measurement of quantitative respiratory carbon-14 patterns and their correlation with the physiological state has required several steps. We have devised very sensitive equipment that continuously and automatically measures and records breath radioactivity; we have used this equipment in animal studies, and we are now applying it to human clinical work.

The total radioactivity in the breath has been measured by use of ionization chambers and vibrating-reed electrometers. Ionization chambers as large as 20 liters are used, and their sensitivity in detection of the carbon-14 is such that in humans an eight-hour respiratory carbon-14 pattern can usually be measured with one microcurie of a labeled compound. An infrared $CO_2$ analyzer and ratio recorder permits the continuous measurement and recording of total $C^{14}$, % $CO_2$, and $C^{14}/\%CO_2$, i.e., specific activity.

In a representative test with this apparatus the patient, Mr. F., was seated comfortably with the helmet in place and with an airflow of ten liters per minute through the system. After the $CO_2$ and the radioactivity background rates had been allowed to equilibrate, the $C^{14}$ background was subtracted. Mr. F. was then injected intravenously with 100 μc of glycine-2-$C^{14}$ and the excretion pattern was recorded for about one hour. Radioactivity appeared in the breath quite rapidly. Within 3 minutes after injection a detectable amount was being excreted, and the peak excretion rate was reached within 30 to 35 minutes, showing that the enzyme systems which take the methylene group of glycine to $CO_2$ work very rapidly. Two more records of one hour each were made during the first day, making extrapolation of the other portion of the curve quite easy. The excretion pattern was then followed at intervals over a period of two weeks. Results are shown in Figs. 1, 2, 3, and 4. Figures 1 and 2 show the rate of excretion in millimicrocuries per g carbon per minute; two different time scales are presented. Figures 3 and 4 show the cumulative excretion of $C^{14}O_2$, using two different time scales on the graphs.

For comparison purposes we have also included the rate and cumulative excretion curves for $C^{14}O_2$ for a rat given glycine-2-$C^{14}$ intraperitoneally (Figs. 5 and 6). The similarities between the human and rat curves are more striking than the dissimilarities; part of the difference could be due to the different methods of injection. These striking similarities would indicate that in the oxidation to $C^{14}O_2$ of the glycine, enzyme reaction rates are slower than circulation, mixing, and absorption rates, and that these enzyme reaction rates are rather comparable in the rat and the human.

The $CO_2$ excretion by Mr. F. has been remarkably constant and has averaged 0.109 g carbon per minute or equivalent to 1.79 g $BaCO_3$/min.

This specific-oxidation-rate apparatus functioned very satisfactorily. A patient could be kept comfortably in the machine for several hours at a time. The sensitivity was excellent -- an eight-hour excretion curve could be measured for a rapidly metabolized compound such as acetate or glucose with an injected dose of 1 μc of $C^{14}$. Two to 5 μc of injected glycine-2-$C^{14}$ would permit measurement of an eight-hour excretion curve.

This great sensitivity makes possible safe oxidation-metabolism studies of specific compounds in noncancer humans. One can consider clinical tests and studies of over-all metabolic abnormalities, such as induced by thyroid disfunction, advanced cancer, nutritional deficiencies, aging effects and drugs.

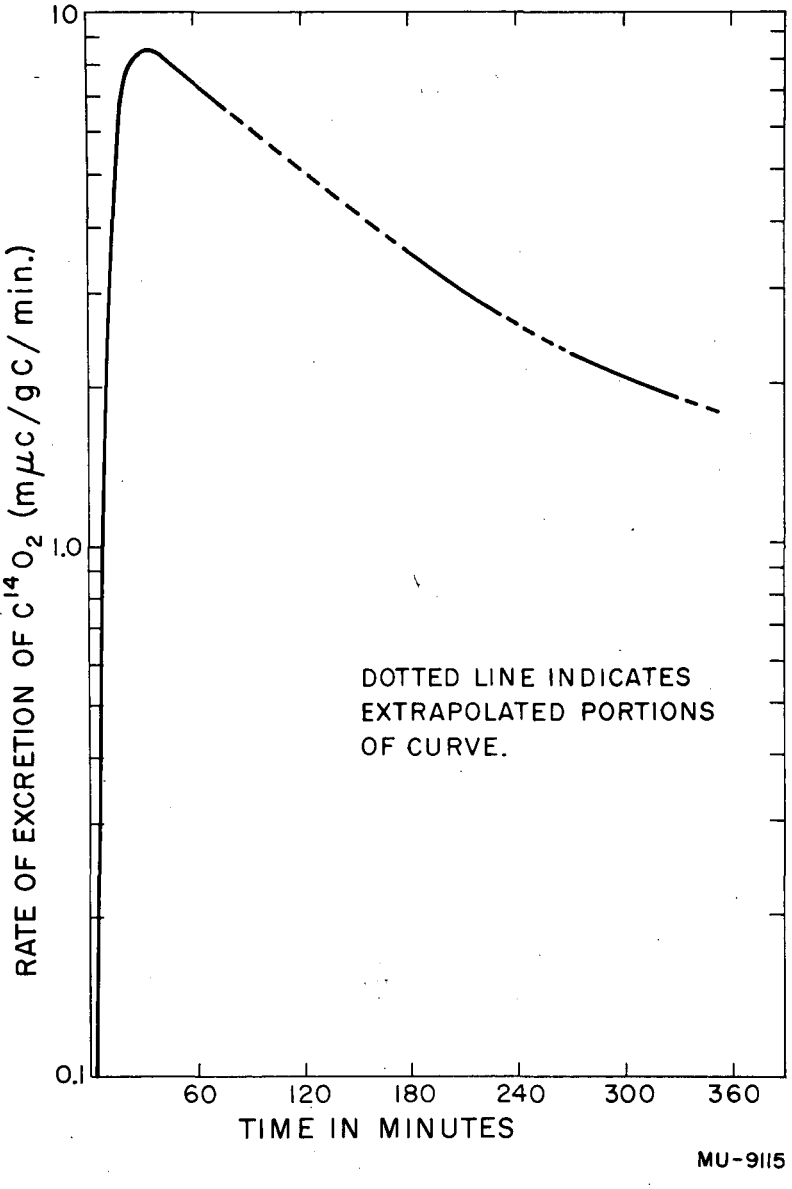


Fig. 1. Rate of metabolism of glycine-2-$C^{14}$ to $C^{14}O_2$ in Mr. F.

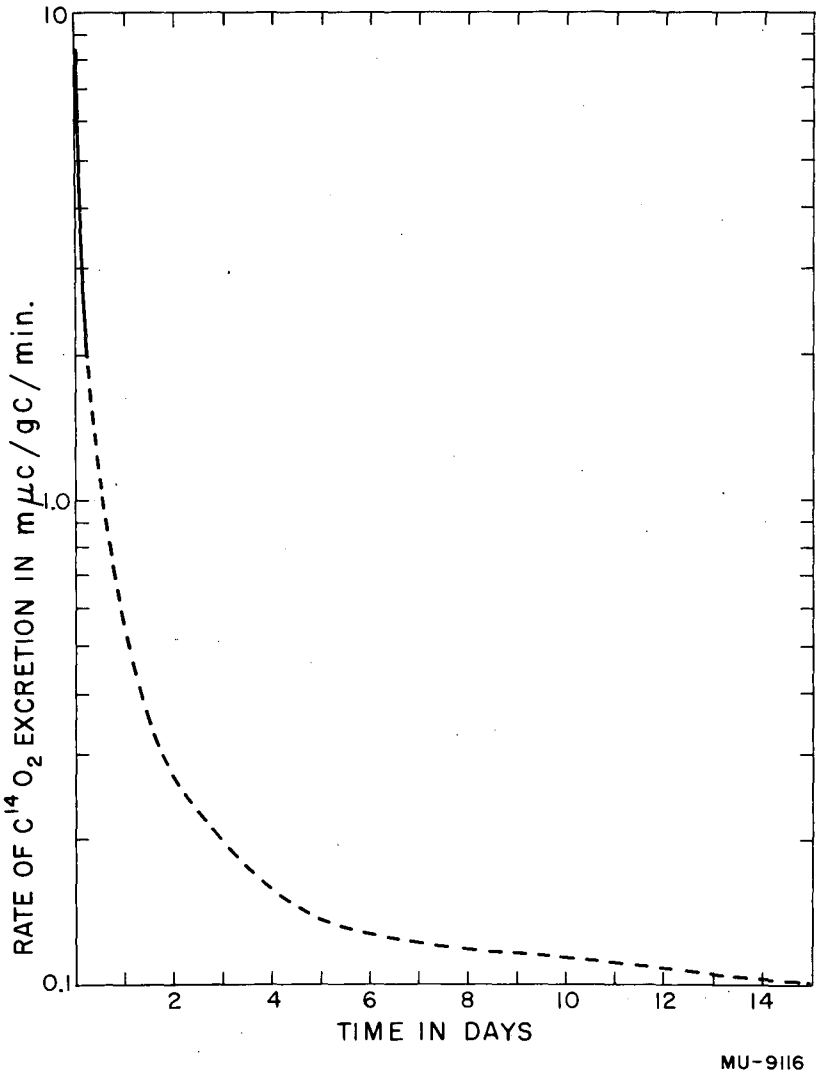


Fig. 2. Rate of metabolism of glycine-2-$C^{14}$ to $C^{14}O_2$ in Mr. F.

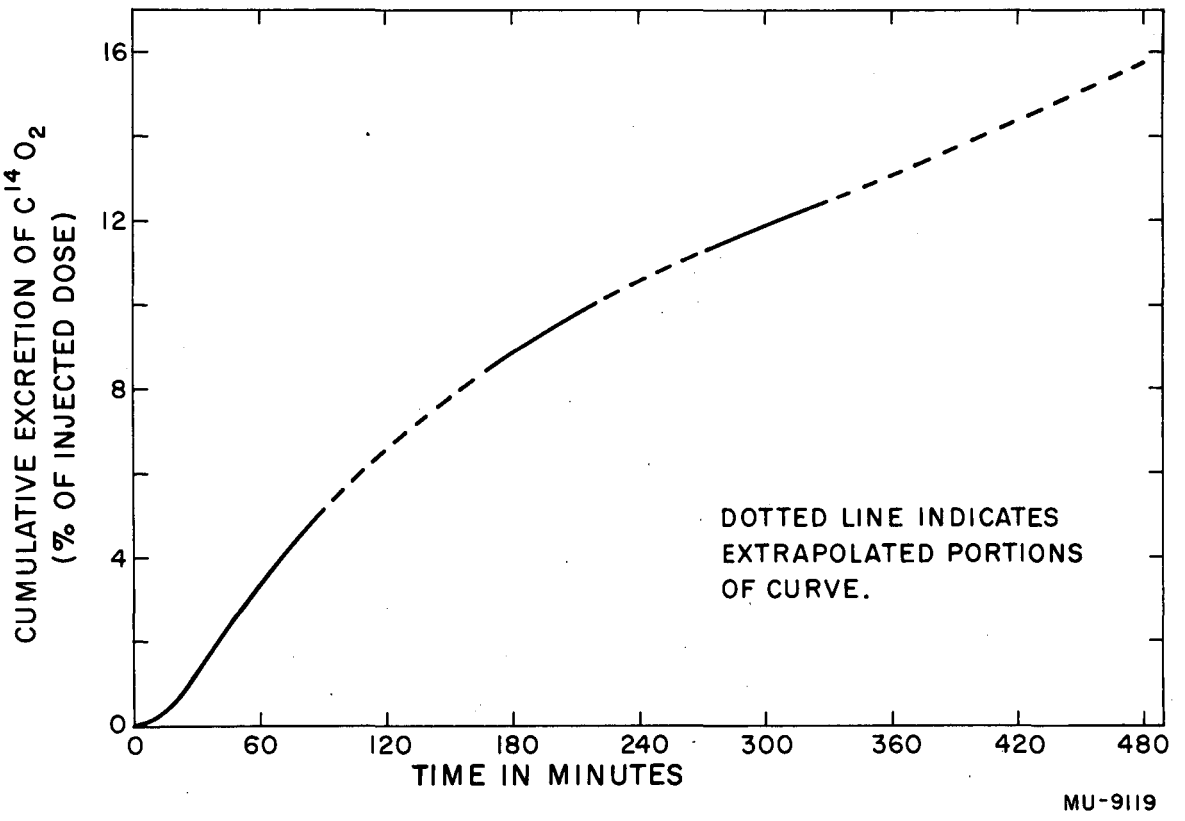


Fig. 3. Cumulative excretion of $C^{14}O_2$ from Mr. F. after injection of 100 μc glycine-2-$C^{14}$.

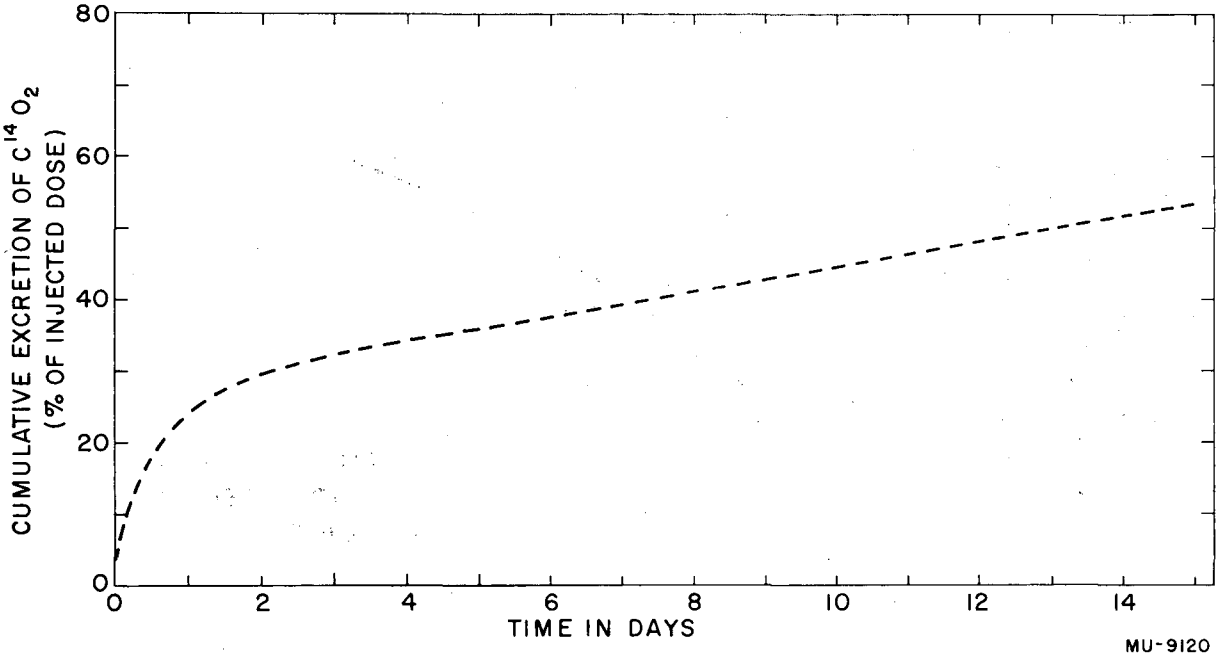


Fig. 4. Cumulative excretion of $C^{14}O_2$ from Mr. F. after injection of 100 μc of glycine-2-$C^{14}$.

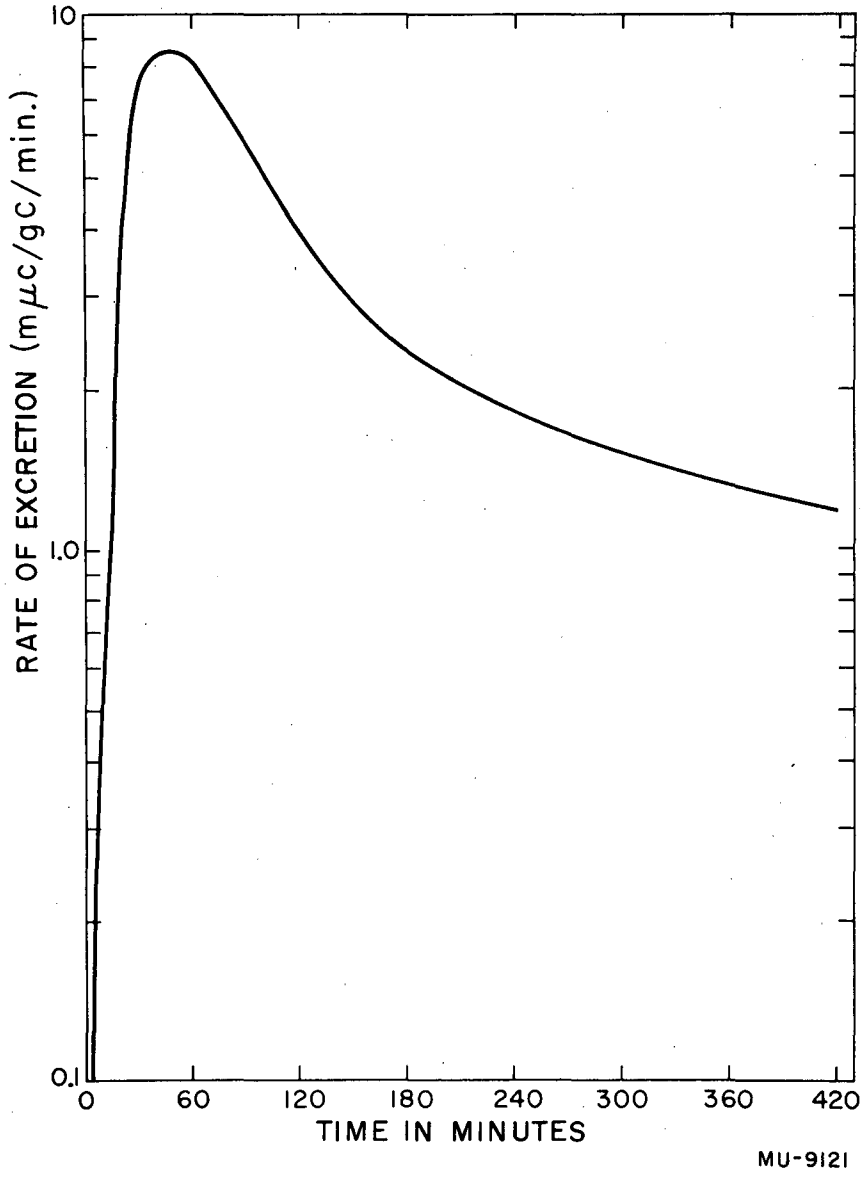


Fig. 5. Rate of metabolism of glycine-2-$C^{14}$ to $C^{14}O_2$ in a Rat.

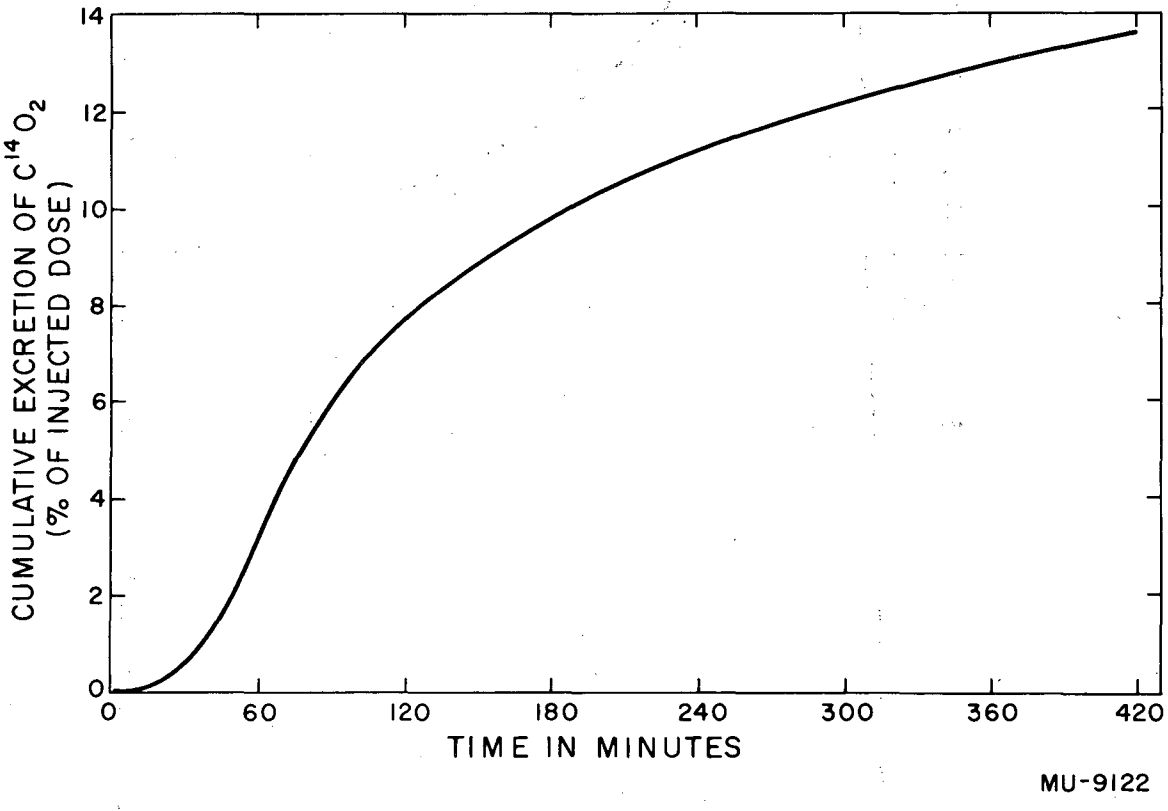


Fig. 6. Cumulative excretion of $C^{14}O_2$ from a rat injected with glycine-2-$C^{14}$. Intraperitoneal injection.

## RESPIRATORY CARBON-14 PATTERNS IN STARVED RATS

Martha R. Kirk, Denham Harmon, and B. M. Tolbert

This study deals with the effect of starvation on the respiratory carbon-14 patterns of rats, and uses acetate-2-$C^{14}$, glucose-$C^{14}_6$, and glycine-2-$C^{14}$ as substrates. The equipment used is that described in a previous quarterly report (UCRL-2647, July 8, 1954), and the unit measures and records continuously the respiratory $C^{14}$, $\%CO_2$, and $C^{14}/\%CO_2$, i.e., specific activity.

Three 325 to 350-g Long-Evans male rats were used for this series--one for each of the compounds studied. A normal respiratory pattern was determined for each animal, after which all food was removed but the animal was allowed water ad lib. Animals survived from 11 to 15 days after food was removed, during which time additional respiratory $C^{14}$ patterns were made for the three substrates at 3- to 5-day intervals.

Graphs in Figs. 7 and 8 show changes in the utilization of glucose-$C^{14}_6$ as starvation progressed, and pertinent data for all compounds are given in Table I.

The rate of utilization of acetate-2-$C^{14}$ seems to change very little with starvation, but the general slowing down of all body processes is reflected in the utilization of both glucose-$C^{14}_6$ and glycine-2-$C^{14}$. In the final stages of starvation the rat seems to be using virtually nothing for body pools. Loss of weight and lowered $CO_2$ production substantiate these observations.

## FURTHER RESPIRATORY CARBON-14 PATTERNS IN RATS

Ann M. Hughes, John Weaver, and B. M. Tolbert

In the general study of the metabolism of labeled compounds to $C^{14}O_2$ using the automatic recording apparatus previously described (UCRL-2531, April 1, 1954), three types of experimentation are currently being explored, viz: (a) the metabolism of a variety of fatty acids in normal rats; (b) the effects of chronic nicotinism on acetate metabolism; and (c) a geriatrics study which will include changes in the metabolism of fats, carbohydrates, and amino acids with increasing age. The geriatrics study is in the preliminary stages, and is not reported at this time.

### Propionate Patterns

To continue the study of the metabolism of fatty acids -- which so far has used sodium acetate-2-$C^{14}$ and sodium heptanoate-7-$C^{14}$ -- the respiratory pattern of sodium propionate, labeled in each of the three carbons, was measured. About 5 μc (2 mg) of the labeled propionate was injected intraperitoneally into young adult male rats. The cumulative excretion and rate of excretion of $C^{14}O_2$ for the three compounds are shown in Figs. 9 and 10, respectively. As was expected, the rate of oxidation of the carboxyl group to $CO_2$ is much faster than the rate of oxidation of the other two carbon atoms, by a factor of about 3. These data are consistent with the work of Lorber

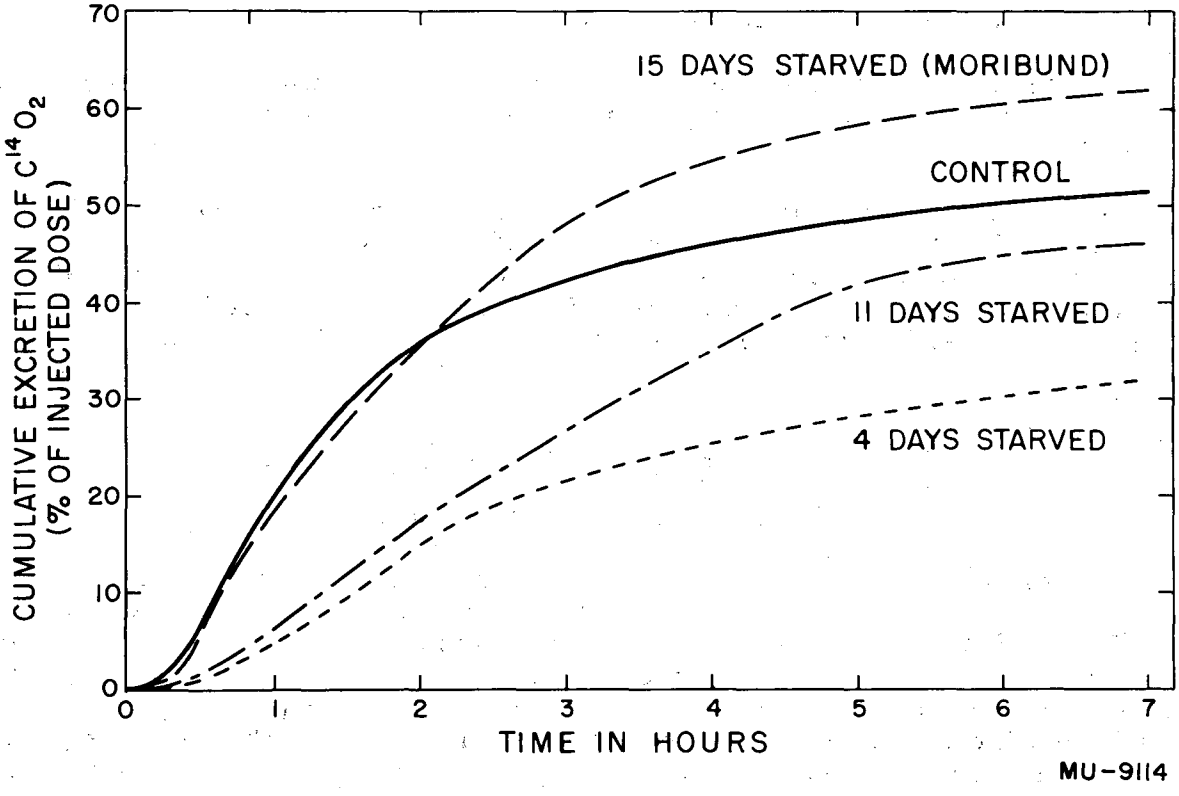


Fig. 7. Cumulative excretion of $C^{14}O_2$ from a rat injected with glucose-$C^{14}_6$. Changes caused by starvation.

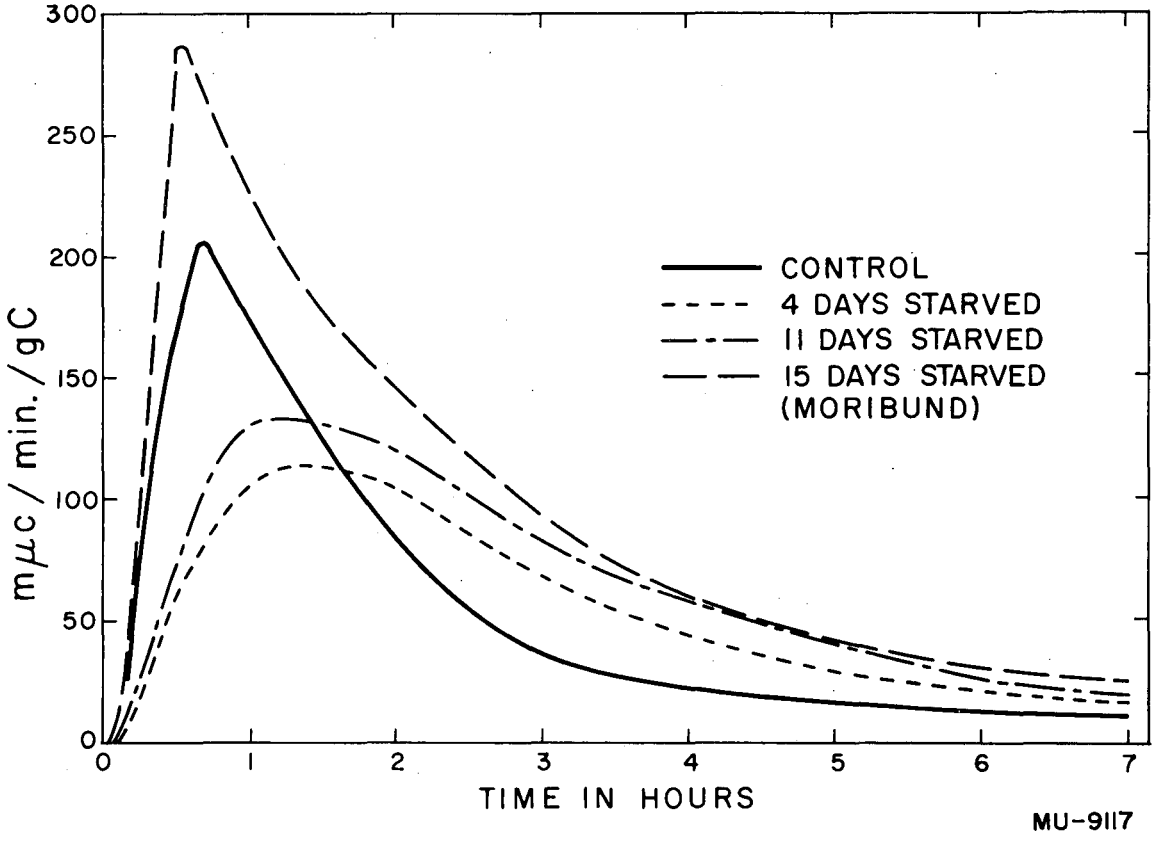


Fig. 8. Rate of excretion of $C^{14}O_2$ from a rat injected with acetate-2-$C^{14}$ expressed as mμc per g carbon per min. Normalized to 10 μc injected dose and 250 g rat. Changes caused by starvation.

Table I

Respiratory Pattern Changes in Starved Rats

| | Weight (g) | $CO_2$/min. (mg) | $CO_2$/min./ 100 g body weight (mg) | $C^{14}$ in* 7 hrs.* (%) | max.sp.act. (mμc per g C/min**) | Time of max.sp.act. (min. after inj.) |
|---|---|---|---|---|---|---|
| Substrate: Acetate-2-$C^{14}$ | | | | | | |
| Control | 347 | 10.22 | 2.95 | 60.21 | 291 | 30 |
| 3 days starved | 317 | 6.64 | 2.09 | 57.09 | 302 | 30 |
| 9 " " | 253 | 5.78 | 2.28 | 59.19 | 302 | 25 |
| 14 " " | 195 | Died | | | | |
| Substrate: Glucose $C^{14}_6$ | | | | | | |
| Control | 323 | 9.78 | 3.03 | 51.26 | 207 | 41 |
| 4 days starved | 270 | 5.94 | 2.20 | 31.95 | 113 | 90 |
| 7 " " | 248 | 6.37 | 2.57 | 42.09 | 121 | 86 |
| 11 " " | 221 | 5.36 | 2.43 | 45.94 | 131 | 60-90 |
| 15 " " | 177 | 3.92 | 2.21 | 64.1 | 287 | 34 |
| Substrate: Glycine-2-$C^{14}$ | | | | | | |
| Control | 363 | 13.96 | 3.85 | 13.61 | 36 | 40-50 |
| 5 days starved | 284 | 7.43 | 2.62 | 13.65 | 42 | 30 |
| 8 " " | 253 | 5.96 | 2.36 | 19.26 | 85 | 30 |
| 11 " " | 212 | 1.77 | 0.83 | 28.85 | 195 | 90 |

* Percent of injected radioactivity.
** Normalized to 10 μc injected dose and 250 g animal.

Calvin

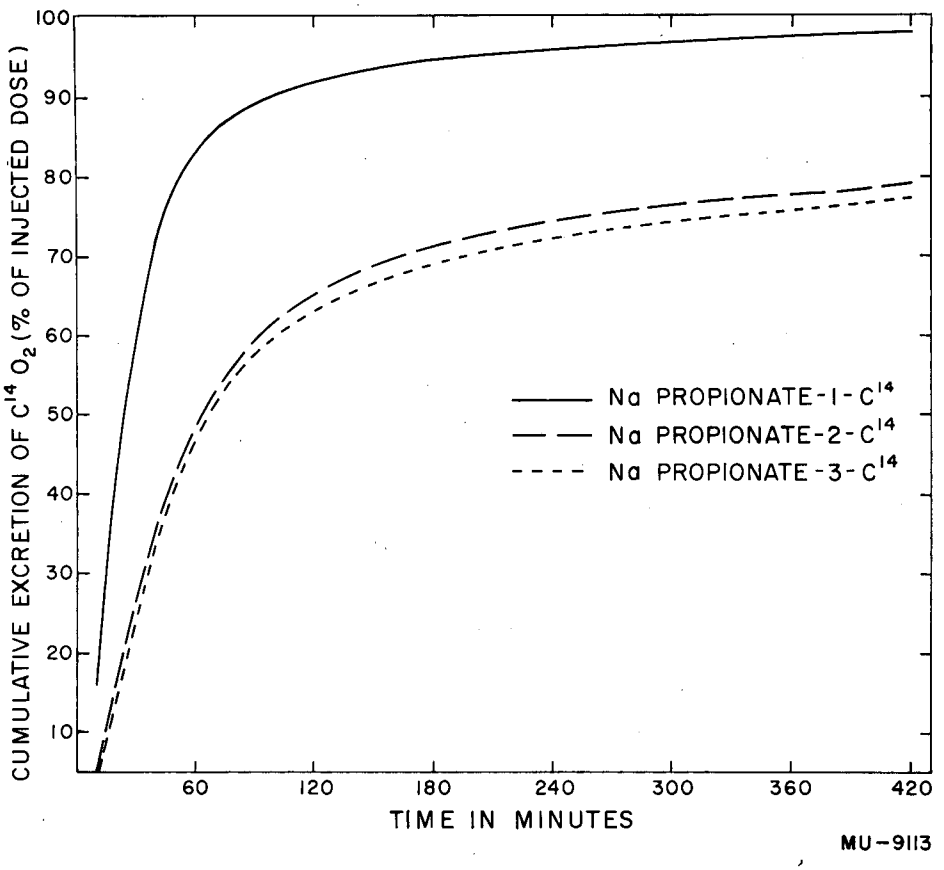


Fig. 9. Cumulative excretion of sodium propionate-$C^{14}$ labeled in the 1, 2 and 3 positions.

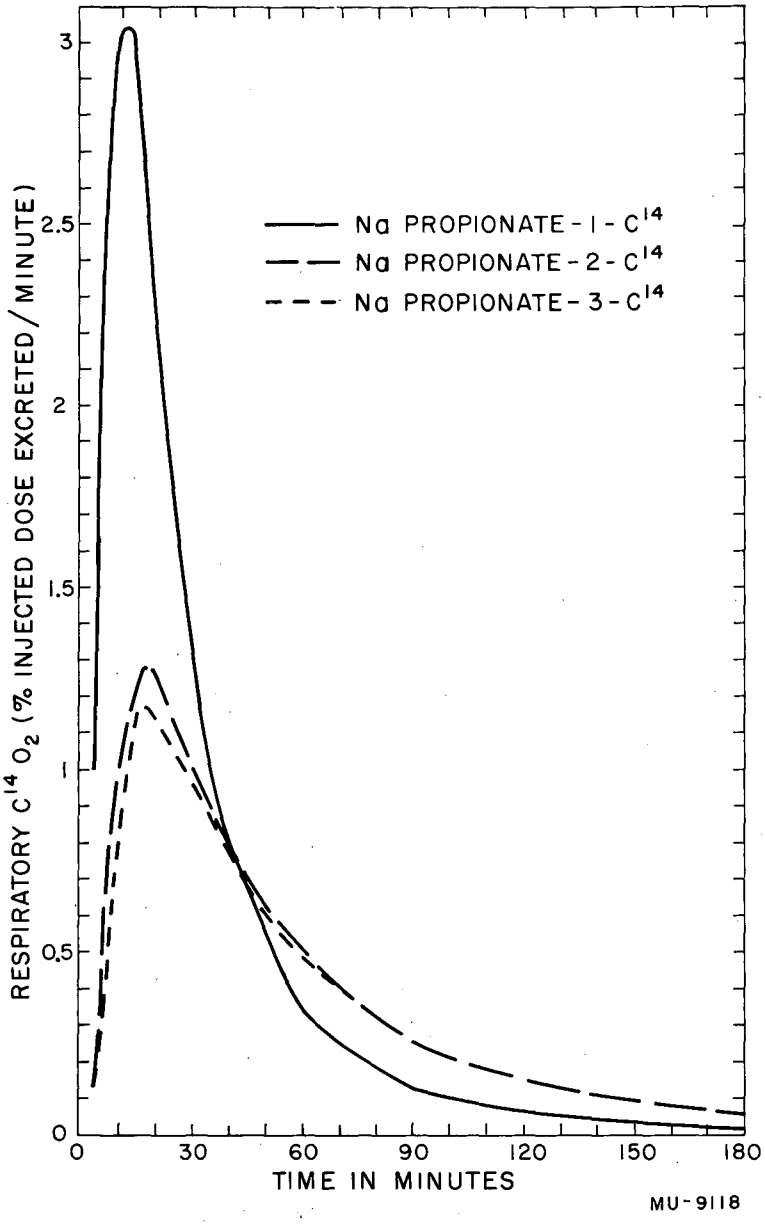


Fig. 10. Rate of excretion of sodium propionate-$C^{14}$ labeled in the 1, 2, and 3 positions.

et al.,[1] in which β-oxidation of propionate to malonate was ruled out by isotopic experiments. The great similarity in both the rate and the cumulative curves for the 2- and 3-labeled propionate is also consistent with previous work, which has shown α-β randomization by the time oxidized propionate appears as lactate or liver glycogen.[2] The somewhat greater rate for the oxidation of the 2-carbon atom of propionate than for the 3-carbon atom indicates that complete randomization of these two atoms does not immediately occur. These data would indicate that propionate is oxidized to a two-carbon fragment, perhaps acetyl-S-CoA, which goes into the citric acid cycle, then back to random α-β-labeled pyruvate and thence to glycogen and lactate.

The agreement between these propionate respiration patterns and the known metabolism of this fatty acid is excellent indication of the potential usefulness of respiratory patterns in biochemical studies.

Nicotine Acetate Patterns

In the preceding quarterly report (UCRL-2841, January 10, 1955) experiments were described in which the acute effects of nicotine administration were studied. No change in the metabolism of acetate to $C^{14}O_2$ following a single injection of nicotine was observed.

In the same report, the beginning of a study of the chronic effects of nicotine was described. At the end of six weeks the rats had developed a tolerance to the original nicotine dose, which was therefore increased to 0.2 mg/g body weight. Beginning during the third week of nicotine administration, determinations of the respiratory metabolism of sodium acetate have been made every other week. Sodium acetate-2-$C^{14}$ (2 mg, about 8 μc) was injected intraperitoneally and the respiratory $C^{14}O_2$ was measured. At the end of fifteen weeks of daily nicotine administration, the injected animals show no consistent significant difference in acetate metabolism from normal litter-mate controls. The animals have been weighed once a week. The average weight curve of the injected animals is gradually falling below that of the normals. This difference did not start to appear until the end of about eight weeks of daily nicotine administration.

## STUDIES ON ADENINE METABOLISM

Edward L. Bennett, Barbara Krueckel, and Martha R. Kirk

As discussed in a previous quarterly report (UCRL-2709, September 30, 1954), the extensive studies of nucleic acid and nucleotide metabolism that have been made with adenine-4,6-$C^{14}$ during the past several years are now being extended to a comparative investigation of the metabolism of adenine-4,6-$C^{14}$, adenine-2-$C^{14}$, and adenine-8-$C^{14}$. Independent metabolism of several of the carbon atoms of adenine, particularly those in the 2 and 8 positions of the purine ring, would appear to be a possibility, according to our present knowledge of the mechanism of nucleotide synthesis and of the role of folic acid

[1] Victor Lorber et al., J. Biol. Chem. 183, 531 (1950).
[2] See loc. cit. and L. Daus, M. Meinke, and M. Calvin, J. Biol. Chem. 196, 77 (1952).

in metabolic pathways concerned with nucleotide biosynthesis.

In these studies, which are not completed, $C_{57}$ male mice have been administered adenine-4,6-$C^{14}$, adenine-2-$C^{14}$, and adenine-8-$C^{14}$. The animals have been sacrificed at intervals up to 28 days after administration of the adenine. In addition, animals receiving adenine-2-$C^{14}$ have also been injected with the folic acid inhibitors, A-methopterin and aminopterin, shortly before the adenine was administered. Preliminary results, subject to revision when the specific activities of the adenine isolated from the soluble nucleotides, RNA, and DNA have been determined, reveal no large differences in the metabolism of adenine-4,6-$C^{14}$, adenine-2-$C^{14}$, or adenine-8-$C^{14}$, nor in the extent of incorporation of adenine-2-$C^{14}$ in normal animals or animals treated with methopterin or aminopterin.

In addition to the incorporation of adenine into nucleotides and nucleic acids, the oxidation of the several labeled carbon atoms to $C^{14}O_2$ and subsequent elimination in the breath has been studied using the continuous respiratory $C^{14}O_2/C^{12}O_2$ analyzer (UCRL-2531, April 1, 1954). If the C-2 or C-8 positions of adenine or compounds derived from it is an equilibrium with the "active formate" pool of the mouse, a relatively large elimination of $C^{14}O_2$ will be observed from adenine labeled in these positions.

As shown in Table II, adenine-2-$C^{14}$, adenine-4,6-$C^{14}$, and adenine-8-$C^{14}$ have markedly different rates of $C^{14}O_2$ excretion. It has been considered that the respiratory $C^{14}O_2$ from adenine-4,6-$C^{14}$ arises from the 6-position during the conversion of the adenine to allantoin. In support of this concept is the fact that no $C^{14}O_2$ is obtained when guanine-4-$C^{14}$ is administered to a mouse, although allantoin is obtained. The respiratory $C^{14}O_2$ from adenine-2-$C^{14}$ and adenine-8-$C^{14}$ must arise from other routes of oxidation. It is interesting to note that little $C^{14}O_2$ is obtained from adenine-2-$C^{14}$ or adenine-8-$C^{14}$ during the first hour or so after administration of the adenine or during the period when a large amount of free adenine is present. Instead, most of the $C^{14}O_2$ arises subsequently when the adenine has been incorporated into nucleotides, nucleic acids, and other compounds which as yet have not been completely identified (UCRL-2647, July 8, 1954). These experiments indicate that either other unrecognized routes of adenine oxidation exist, or the exchange of the 2- and 8-position of the purine ring, as discussed, does in fact occur, particularly after the adenine has been incorporated into nucleotides or nucleic acids. Administration of A-methopterin or aminopterin, however, did not change the $C^{14}O_2$ excretion of adenine-2-$C^{14}$ significantly, as might be expected if folic acid were involved in this formation of respiratory $C^{14}O_2$ from adenine-2-$C^{14}$.

Further analyses of the nucleotide and nucleic acid adenine specific activities of numerous tissues of the mice used in the above experiments are in progress.

Table II

Respiratory $C^{14}O_2$ Obtained After Administration of Adenine-$C^{14}$ to $C_{57}$ Male Mice*

(Cumulative % of Injected Adenine)

| Time (Hr) | Adenine-2-$C^{14}$ (%) | | Adenine-4,6-$C^{14}$ (%) | | Adenine-8-$C^{14}$ (%) |
|---|---|---|---|---|---|
| 0-1 | 0.10 | 0.09 | 0.18 | 0.22 | 0.04 |
| 0-2 | 0.39 | 0.23 | 0.70 | 0.67 | 0.09 |
| 0-4 | 2.0 | 1.3 | 1.9 | 2.0 | 0.37 |
| 0-6 | 3.8 | 2.4 | 2.8 | 3.1 | 0.70 |
| 0-8 | 4.5 | 2.9 | 3.6 | 3.9 | 0.96 |
| 0-12 | 5.3 | 3.6 | 4.7 | 5.2 | 1.3 |
| 0-16 | 5.5 | 4.1 | 5.6 | 6.7 | 1.6 |
| 0-20 | 5.7 | 4.4 | 6.3 | 7.3 | 1.7 |
| 0-22 | 5.8 | 4.5 | 6.6 | 7.5 | 1.73 |

* See also Table I, UCRL-2709, September 30, 1954.

## SYNTHESIS AND RADIATION DECOMPOSITION OF THIOCTIC-$S^{35}{}_2$ ACID

Patricia T. Adams

The synthesis of thioctic acid reported by Reed and Niu[1] presents a satisfactory method of introducing radioactivity into the thioctic acid molecule through the use of sulfur-35. By the following experimental procedure, thioctic-$S^{35}{}_2$ acid has been prepared on a 2.5-millimole scale with a specific activity of 1 μc/mg.

### α-Toluenethiol-$S^{35}$

An ethereal solution of benzylmagnesium chloride (10 millimoles in 25 ml of ether) was added with stirring to a slurry of 160 mg (5 millimoles) of amorphous sulfur containing 0.5 mc of $S^{35}$ in 15 ml of dry benzene. The mixture was heated under reflux for 4 hours, cooled, and treated with water and acid to decompose the Grignard complex. The toluenethiol was extracted into ether solution and this solution was carefully dried over sodium sulfate. An aliquot portion of the ethereal solution was titrated against standardized iodine solution. The yield of thiol was 4.4 millimoles (85%). Attempts to

[1] L. J. Reed and C. Niu, J. Am. Chem. Soc. 77, 416 (1955). See also P. T. Adams, Univ. of Calif. Radiation Laboratory Report No. UCRL-2841, January 10, 1955, p. 25.

isolate this thiol through distillation resulted in loss of product through oxidation to benzyldisulfide.

6, 8-Dibenzylmercapto-$S^{35}_2$-octanoic acid

The ethereal thiol solution was heated at 80° under a nitrogen atmosphere until the volume was reduced to approximately 10 ml. Absolute ethanol (20 ml) was added and the solution was again concentrated to 10 ml. A solution of ethyl-6, 8-dibromooctanoate (738 mg, 2.2 millimoles) in 10 ml of ethanol, followed by 102 mg (4.4 millimoles) freshly cut sodium, was added to the thiol solution. After 4 hours' heating at reflux, a precipitate of sodium bromide had appeared. Potassium hydroxide (340 mg) was added, and the mixture was allowed to stand overnight. The reaction mixture was diluted with water, acidified, and extracted with ether. The ethereal solution was washed with water, dried, and distilled to dryness; the oily residue contained 0.4 mc $S^{35}$. Crystallization of the acid at this point resulted in loss of product and did not improve the yield on subsequent steps. Consequently the crude acid was used for the following reduction.

Thioctic-$S^{35}_2$ Acid: Low Specific Activity

The crude dibenzylmercapto acid was extracted into 5 ml of dry toluene. (A toluene-insoluble polymer contained 0.08 mc, 16% of the starting activity.) This solution was added very slowly with stirring to a solution of sodium in 50 ml of liquid ammonia. Additional pieces of sodium were added to the reaction mixture until a dark blue color was maintained for 30 minutes. At the end of this time the blue color was discharged with ammonium chloride and the ammonia was allowed to evaporate. The residue was dissolved in water and extracted with ether. The clear aqueous solution was diluted to 80 ml and the pH was adjusted to 7.0. One ml of 1% ferric chloride solution was added and oxygen was bubbled through the solution for 20 minutes. The solution was acidified and extracted with chloroform. Evaporation of the chloroform left a viscous yellow oil. The product was extracted into hot hexane, allowed to crystallize, isolated, and recrystallized from hexane. The thioctic acid was isolated as light yellow crystals. The pure product weighed 54 mg (10% yield from $S^{35}$) and had a specific activity of 1.12 μc/mg (theory, 1.0 μc/mg). The compound showed the characteristic ultraviolet absorption spectrum with $\lambda_{min}$: 280mμ; $\lambda_{max}$: 333 mμ; $\epsilon_{max}$: 149.

Thioctic-$S^{35}_2$ Acid: High Specific Activity

Following the experimental procedure detailed above, 3 preparations of thioctic-$S^{35}_2$ acid (specific activity 1 μc/mg) were completed with over-all yields of 8%, 10%, and 16%. In order to obtain material more useful for biological experiments, a synthesis utilizing 200 mc $S^{35}$ (specific activity of product = 200 μc/mg) was undertaken. The yield of α-toluenethiol was 88%. The crude dibenzylmercaptooctanoic acid contained 150 mc (75%). Sodium-ammonia reduction, followed by oxygen oxidation to the disulfide, proceeded smoothly to give a yellow oil product just as in preceding preparations. However, repeated attempts to obtain crystalline thioctic acid from this oil by hexane extraction and crystallization failed. A perfectly clear hot hexane solution of the radioactive thioctic acid was allowed to cool for several hours. A large percentage of the oily product that separated from the cool hexane

would not redissolve in hot hexane. With each attempt at crystallization, more of this insoluble oil was formed. Since these crystallization attempts were identical to those successfully employed in isolating the less radioactive acid, it was concluded that radiation from the $S^{35}$ was destroying the product in solution so rapidly that crystallization was impossible.

It was found that a solution containing thioctic acid with no radioactive impurities could be obtained in the following manner. The combined oily products from several crystallization attempts were extracted with 4 small portions of hot hexane, leaving behind a large insoluble residue. This residue, examined spectrophotometrically, was found to contain almost no thioctic acid. The hexane extract, containing 3.6 mc $S^{35}$, was immediately evaporated to dryness and extracted with several small portions of 0.01 M phosphate buffer (pH 6.75). Again a large residue remained. This residue contained 2.5 mc $S^{35}$ of which about 25% was thioctic acid, 25% was thioctic acid sulfoxide, and 50% was a radioactive compound not yet identified.

Analysis of the buffer solution by one-dimensional paper chromatography (with butanol-N/2 ammonium hydroxide as solvent) showed 6% of the radioactivity on the origin, 7% as thioctic acid sulfoxide ($R_f$ 0.25), and the remainder as thioctic acid ($R_f$ 0.5), with no other radioactive impurity. This solution (1.1 mc) was used for the biological experiments described elsewhere.

A check on the chromatographic behavior of thioctic acid was made, using spectroscopically pure crystalline acid (1.1 μc/mg). Three spots invariably appear, with the relative amounts varying with the solvent system used. In butanol-ammonia (N/2) solvent, the sulfoxide spot contains 4% to 8%, the origin contains 5% to 15%, and the thioctic acid spot contains the remainder of the activity. Percentages of both of the derivative compounds increase when the thioctic acid applied to the origin is heated or allowed to stand in air before introduction of the solvent.

## Radiation Decomposition of Thioctic Acid

Samples of thioctic acid have been subjected to γ-irradiation from a $Co^{60}$ source. The rate of decomposition measured is quite normal for organic compounds: for crystalline thioctic acid, $G = \frac{\text{molecules decomposed}}{100 \text{ ev absorbed}} = 10$; for a $7 \times 10^{-3}$ M hexane solution, G = 8.7. With the sulfur-35 β-radiation producing $3 \times 10^{16}$ ev/day/mg of the high-specific-activity thioctic acid, we calculate a decomposition rate of 0.1%/day, using G = 10 from the γ-irradiation experiment. It appears that the self-decomposition rate is greater than this.

Investigation into the nature of the decomposition of the product in the high-specific-activity synthesis is under way.

## 6-METHYLMORPHINE

Helen N. Reist and Henry Rapoport

The recent discovery of the oxidation of codeine to codeinone by silver carbonate in benzene suggested the possible application of this procedure to the preparation of morphinone and 6-methylmorphine. Neither compound has been reported in the literature and both would be interesting to test pharmacologically. This report is concerned with the preparation of 6-methylmorphine.

Before oxidation of the 6-hydroxy group of morphine could be undertaken, it was necessary to block the phenolic 3-hydroxyl by a group which could subsequently be easily removed. Such a blocking agent is the methoxymethyl group, and 3-methoxymethylmorphine was prepared from sodium morphinate and chloromethyl ether following known procedures. Oxidation with silver carbonate in refluxing benzene then gave a 41% yield of methoxymethylmorphinone, mp 126°–129°, from benzene-hexane; $[\alpha]_D^{25}$ -176° (c, 0.98, ethanol). With sodium borohydride, this ketone was easily reduced back to methoxymethylmorphine, and with methyllithium it gave 6-methylmethoxymethylmorphine. The latter compound was hydrolyzed with acetic acid to 6-methylmorphine, mp 279°–280° after crystallization from butanone. With diazomethane, 6-methylmorphine was converted to the known 6-methylcodeine. A sample of 6-methylmorphine has been submitted to Dr. N. B. Eddy at the National Institutes of Health for testing.

## EQUIPMENT FOR ELECTRON IRRADIATIONS

Richard M. Lemmon and Duane Mosier

An improved apparatus for the electron irradiation of organic compounds has been put into operation. As was previously reported (UCRL-2647, July 8, 1954), the system that had been in use for measuring electron dosages was subject to large errors due to (a) stoppage of some electrons by the sample itself and by the glass walls of the sample container, (b) scattering of electrons by the sample and container, (c) secondary electron emission, and (d) air ionization. These errors have now been largely eliminated by the new arrangement, which includes the following features (see Figs. 11 and 12):

1. The electron beam (A) from the linear accelerator is passed under high vacuum ($10^{-6}$ mm Hg) through a magnetic field of 1500-gauss strength (B). The use of the magnetic field gives a monoenergetic beam (approximately 0.1 μamp) of about 4.5 Mev. This beam is of sufficient energy to pass entirely through both holder and sample with negligible stoppage of electrons.
2. After emerging from the magnetic field, the electron beam passes through an aluminum collimator (D), which is 13 mm in length and has a 6-mm inside diameter, and into a cylindrical vacuum tank (C). This tank, which is about 13 cm in diameter and 23 cm in length, is also maintained at a vacuum of $10^{-6}$ mm Hg during irradiations. After traveling 76 cm, the beam then passes through a second aluminum collimator (E, 12 mm in length and 9 mm inside diameter), which is clamped to the sample holder. Immediately behind the second collimator is the flat-sided irradiation section of the glass sample holder (F), which is about 10 to 12 mm in cross-section area. Just behind

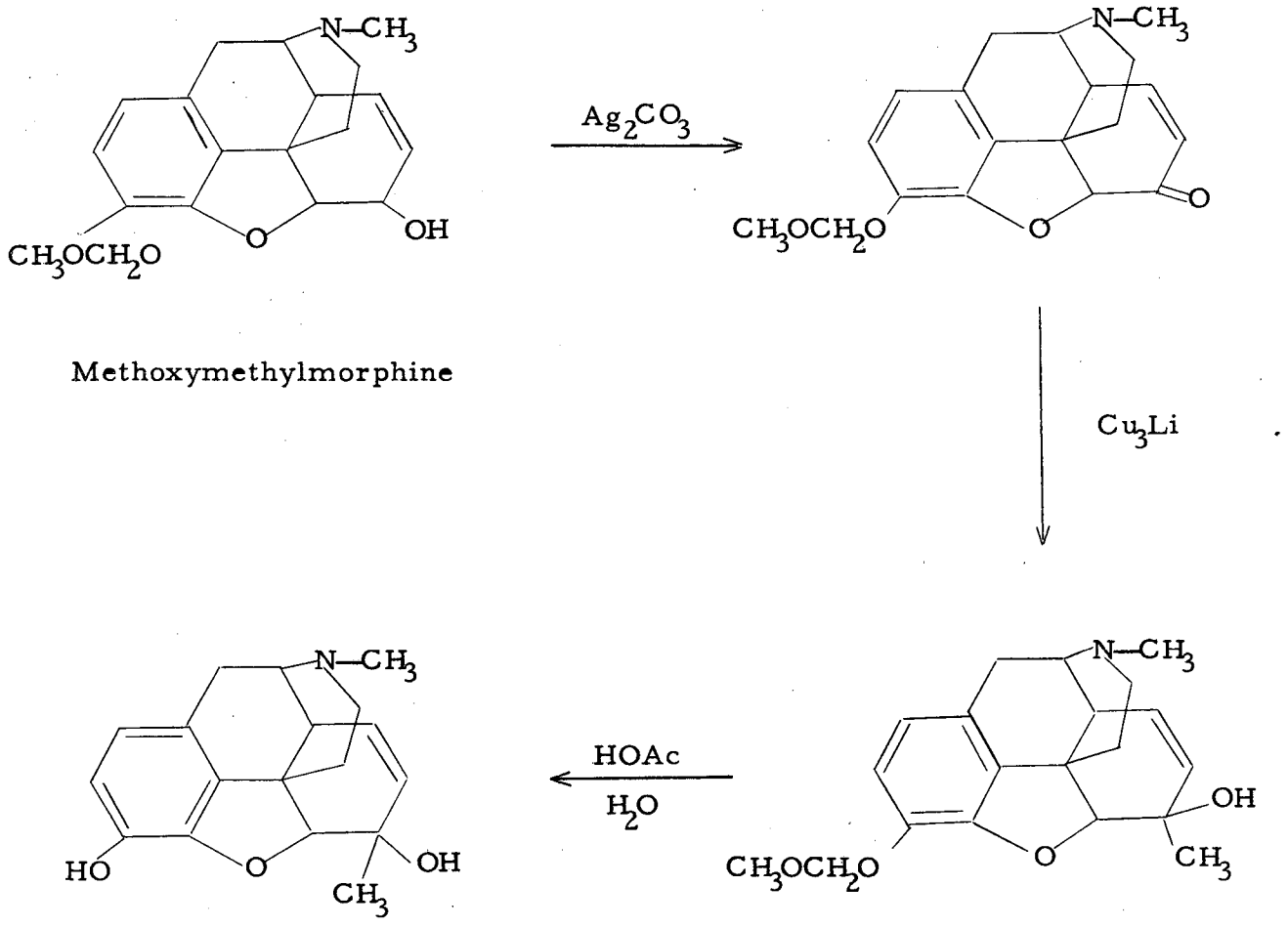


Methoxymethylmorphine

6-Methylmorphine

Calvin

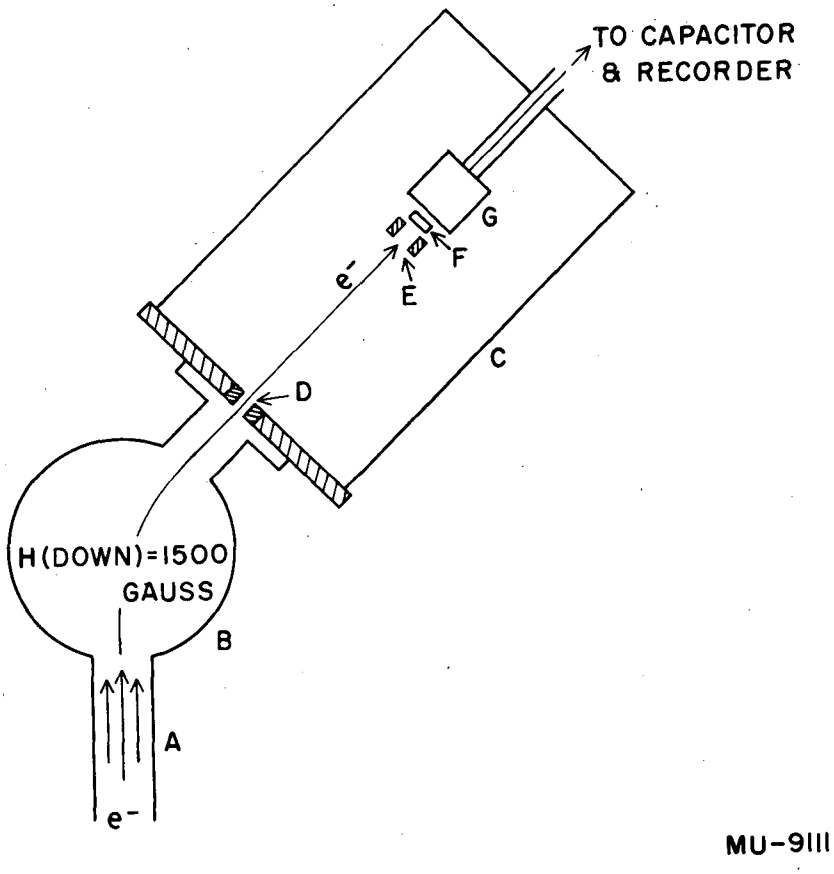


Fig. 11. Apparatus for high-energy electron irradiations (top view).

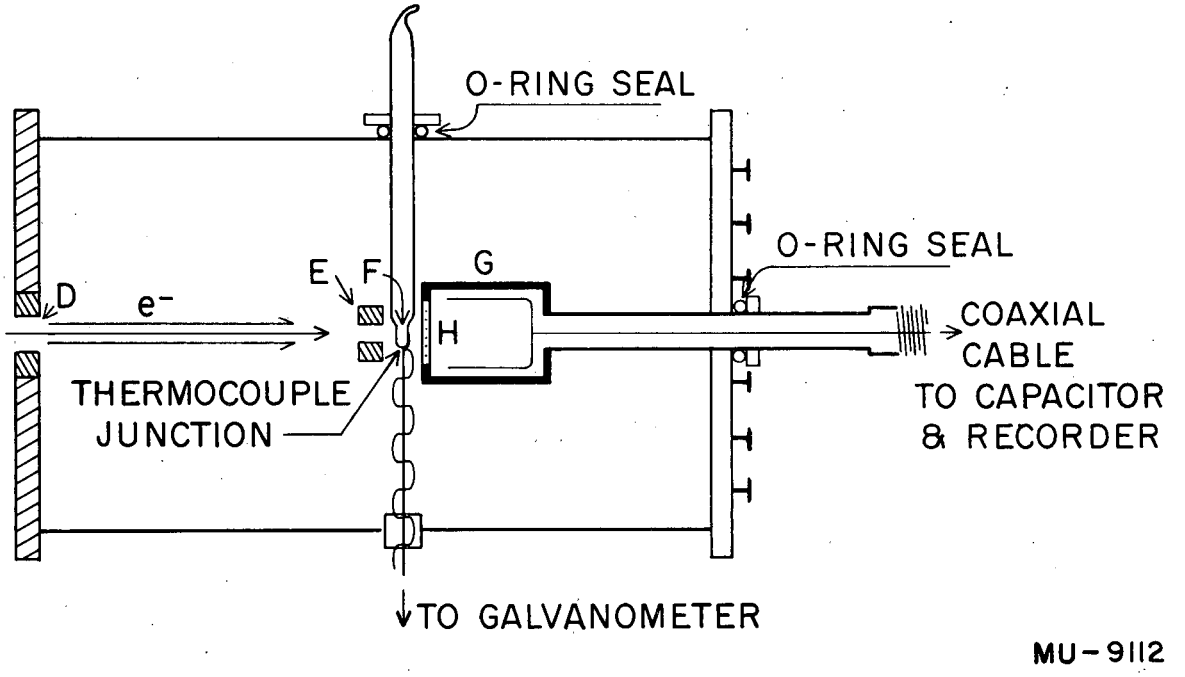


Fig. 12. Vacuum tank for high-energy electron irradiations (side view).

the sample holder is a Faraday cup or electron collector (G). Since the tank is under high vacuum there is no problem of air ionization, and there is very little spreading of the electron beam before it reaches the sample holder. The electrons are scattered in passing through the holder and sample but the Faraday cup is large enough, and close enough to the holder, to collect nearly all these electrons. With the electron beam turned on, the presence or absence of the holder and sample makes no detectable difference in the rate at which electrons are collected in the Faraday cup.

3. A grid of 10 strands of 10-mil tungsten wire (H) is placed at the front of the Faraday cup for the purpose of repelling secondary electrons. A negative charge of 100 to 300 volts from a power supply is placed on this grid during irradiations. It has been observed, however, that the presence or absence of this charge during irradiations causes no difference in the rate of electron collection in the Faraday cup.

4. The temperature reached by the sample is measured by an iron-constantan thermocouple (Fig. 12) which is attached directly to the glass of the sample holder by means of sealing wax. During irradiations the intensity of the electron beam was kept at such a level that the samples were never heated above 45°.

5. The electrons collected by the Faraday cup are led to a 0.1-μfarad capacitor, which is connected to a Leeds and Northrup "Speedomax" recorder. When the capacitor reaches a charge of 10 volts it is automatically discharged. Each discharge is equivalent to the collection of 1 μcoulomb of electrons on the Faraday cup; the number of these discharges can be read from the recorder.

The efficiency of the electron-beam collimation was tested by placing a simulated sample holder made of brass, of exactly the same size as the glass sample holder, in the usual position behind the second collimator. The greater density of the brass, however, enables the brass "holder" to stop electrons up to about 6 Mev energy. This "holder" was found to stop 93% of the electrons from reaching the Faraday cup. The 7% that reached the cup were due to "fringing" off the walls of the second collimator, which enabled some of the electrons to reach the cup without passing through the sample. Therefore, the number of electrons reaching the Faraday cup when a sample was in place was always multiplied by 0.93 to get the number of electrons actually passing through the sample.

The energy given to the sample per electron is obtained by applying Feather's Rule:

Energy Loss in Mev/electron = $\Delta E = \frac{\Delta R}{0.54}$, where R is the range in $g/cm^2$. The calculation of the energy received by the sample is calculated as follows:

Since there are $5.2 \times 10^7$ Mev/g/rep,

$$\text{rep received by sample} = \frac{(\text{no. of electrons})(\Delta E)}{(\text{grams})(5.2 \times 10^7)}$$

$$= \frac{(\text{coulombs})(6.2 \times 10^{18}\ \text{electrons/coulomb})(\Delta R)}{(\text{grams})(5.2 \times 10^{7})(0.54)}$$

$$= \frac{(\text{coulombs})(2.2 \times 10^{11})}{\text{cm}^2}$$

The $cm^2$ referred to in this calculation is the area of the flat sides of the irradiation section of the sample holder. This calculation assumes that the electron beam is of uniform density throughout this area, an assumption that is not quite correct since the diameter of the beam is some 2 to 4 mm less than that of the irradiation section. This difference, however, introduces only a very small error into the calculation. It is probable that the method outlined above for the calculations of electron-beam dosages is valid to within ±20%.

## EFFECTS OF IONIZING RADIATION ON CHOLINE CHLORIDE AND ITS ANALOGS

Richard M. Lemmon and Margaret A. Parsons

A number of compounds have been irradiated using the improved electron beam apparatus described above. The glass tubes that held the samples during the irradiations are the same as were described in the earlier report (UCRL-2647, July 8, 1954). The samples were dried under high vacuum for 2 to 4 hours at 80°–100° before the tubes were sealed. Therefore, the crystalline samples were completely free of water and oxygen during the irradiations. The determinations of the amounts of decomposition were also made in the manner described in the same earlier report (Reinecke salt precipitations).

Table III lists the choline analogs that have been irradiated with the new apparatus and the G values obtained.

The G value for choline chloride (av = 84) appears far higher than that (about 20) reported earlier (UCRL-2647, July 8, 1954) using the less precise method of dose measurement. It is possible, however, that this discrepancy, and some of the other discrepancies appearing in Table III, may be due to an effect of the rate of energy input. The G values of about 20 for choline chloride were obtained from irradiations that lasted about 10 minutes; the choline chloride irradiations described in this report lasted from 40 to 80 minutes. A yet slower input of energy, namely γ-irradiations lasting about one week, give choline chloride G values in the neighborhood of 200. The self-irradiation of $C^{14}$-labeled choline chloride (irradiations lasting several months) give G values around 1,000. The dependence of G values on the rate of energy input will be the subject of a forthcoming investigation.

The data presented in Table IV for choline bromide indicate that, after choline chloride, the bromide is the most radiation-sensitive of the choline analogs. Data on the γ-irradiation of choline bromide (UCRL-2841, January 10, 1955) have also led to the same conclusion.

Table III

Electron Decomposition of Choline Analogs

| Compound | Rep $\times 10^{-6}$ | % Decomp. | G Value* (molecules decomp. per 100 ev) |
|---|---|---|---|
| Choline chloride | 9.4 | 12 | 106 |
| " | 9.9 | 6 | 50 |
| " | 15.9 | 15 | 78 |
| " | 33.5 | 24 | 59 |
| " | 10.4 | 16 | 127 |
| Choline bromide | 36.5 | 45 | 79 |
| " | 6.9 | 4 | 37 |
| " | 13.7 | 7 | 32 |
| " | 19.8 | 8 | 25 |
| Choline iodide | 62.2 | 2 | 1.6 |
| " | 143 | 4 | 1.4 |
| Choline nitrate | 68.2 | 0 | <1 |
| " | 66.0 | 1 | 1.1 |
| Choline sulfate | 17.5 | 4 | 17 |
| " | 39.5 | 6 | 12 |
| $[(CH_3)_2\overset{C_2H_5}{\overset{\vert}{N}}CH_2CH_2OH]^+Cl^-$ | 20.6 | 3 | 11 |
| " | 49.7 | 8 | 12 |
| " | 46.2 | 6 | 10 |
| $[(C_2H_5)_2\overset{CH_3}{\overset{\vert}{N}}CH_2CH_2OH]^+Cl^-$ | 14.7 | 5 | 23 |
| " | 29.8 | 5 | 12 |
| " | 43.5 | 4 | 6 |

* Determined by Reineckate precipitation of the unchanged product.

## IRRADIATION CHEMISTRY OF dl-METHIONINE

Robert M. Noller and B. M. Tolbert

A 584-mg sample of dl-methionine was irradiated in the 100-curie $Co^{60}$ source. It received $9.3 \times 10^7$ rep at the rate of $3.0 \times 10^5$ r/hr. The sample tube was subsequently sealed to a Toepler pump system and the gases, volatile at room temperature, were collected for measurement and analysis.

The principal gaseous products were $78 \times 10^{-4}$ mM $H_2$, $167 \times 10^{-4}$ mM $CH_4$, $324 \times 10^{-4}$ mM $CO_2$, and $44 \times 10^{-4}$ mM of an unknown material. There was no indication of any $NH_3$. Another sample, however, which received $1.5 \times 10^8$ rep, was heated to 70°C while being evacuated. The analysis has not been completed, but there is $NH_3$ present in addition to $CH_3SH$, and $CH_3SCH_3$. G values for the production of $CO_2$ and $CH_4$ are respectively 0.62 and 0.32. If the $CO_2$ and $CH_4$ are formed by separate processes, then a minimum value for the $G_{decomp.}$ would be equal to $G_{CO_2} + G_{CH_4}$, i.e., 0.94.

The irradiated material, after having volatile products removed, gives a positive nitroprusside test. Pretreatment with sodium amalgam does not increase the color intensity. This indicates that there are sulfhydryl groups present but no large amounts of disulfides.

## PHOTOSYNTHETIC FORMATION OF AMINO ACIDS FROM FORMALDEHYDE AND POTASSIUM NITRATE

Rosemarie Ostwald

There have been many speculations concerning the origin of life. Recently experiments have been reported intending to show that amino acids, smallest building blocks of proteins, can be formed from substances and under conditions presumably present in primordial times. One of these reports[1] describes the formation of amino acids by illumination of a mixture of formaldehyde, potassium nitrate, and ferric chloride. We have attempted to repeat and extend this work.

Mixtures of formaldehyde, potassium nitrate, and ferric chloride were illuminated in quartz cells with a kilowatt mercury-arc lamp for various time intervals. Some experiments were carried out omitting ferric chloride. The solutions were desalted by the consecutive passage through a cation and an anion exchanger and subsequently chromatographed on paper and sprayed with ninhydrin reagent.

The results so far show that there is formation of a mixture of ninhydrin-positive substances, both during short-term illuminations (30 min to 3 hr) in the presence of ferric chloride and during long-term illuminations (20 hr or more) in its absence. It seems that ferric chloride increases the rate of formation of these compounds, so that during long-term illuminations in its presence the reactions have gone further and the ninhydrine-positive substances have been destroyed.

---

[1] K. Bahadner, Nature 173, 1141 (1954).

The nature of these substances is as yet unclear. The color reactions with ninhydrin and with the potassium iodide-starch reagent (as some of the spots on the chromatograms show) indicate that they are α-amino acids, small peptides, or certain amines. There is not much known about the behavior of pyrrolidenones and similar compounds with these reagents.

The behavior of the illuminated solutions on ion-exchange resins shows that they consist of mixtures of substances. The largest part are neutral or acidic compounds, passing through a cation exchanger (Dowex 50 in the hydrogen form). There is an amphoteric fraction held up by both the cation exchanger and an anion exchanger (Dowex a1 in the hydroxyl form). There is also a neutral fraction (passing through the cation and the anion exchanger) and an acidic fraction (passing through the cation exchanger but held up by the anion exchanger). The neutral α-amino acids can only be in the amphoteric fractions, even though the others also contain ninhydrin-positive compounds.

Further work will attempt to identify some of these fractions and individual substances. The working hypothesis is that during illumination pyrrolidenones or similar neutral ring structures are being formed which, during subsequent procedures of ion-exchange passages and heating in acidic media, are split open to form amino acids.

## KINETIC STUDY OF THE ALKALINE HYDROLYSIS OF TRIFLUOROACETYL AMINO ACIDS

Rosemarie Ostwald

This study was undertaken in connection with work designed to develop a peptide synthesis using physiological conditions (aqueous medium and neutral pH). As described by Schallenberg and Calvin,[1] trifluoroacetyl amino acids are easily accessible starting compounds whose protecting group, trifluoroacetic acid, is stable in aqueous solution up to a pH of 8 to 9, and then comes off easily. A kinetic study of the alkaline hydrolysis of a group of trifluoroacetyl amino acids will not only elucidate its mechanism but also allow predictions of the usefulness of the various members of the group for peptide synthesis.

Trifluoroacetylglycine was used in the preliminary experiments. A pH-stat is used to follow the course of hydrolysis. The apparatus plots automatically the amount of alkali added to the reaction mixture necessary to maintain a given pH vs time.

The hydrolyses were carried out at 20°, 30°, and 40°C and at pH 10.0, 10.5, 11.0, and 11.5.

The results show that the reaction is first-order in respect to substrate (straight-line plot of log percent hydrolysis vs time) and in respect to hydroxyl ions (straight-line plot of log k vs pH). The temperature coefficient, $\frac{k_{30}}{k_{20}}$, at pH 11.5, 11.0, and 10.65 is 3.9, 3.3, and 3.1, respectively. The

---

[1] E. Schallenberg and M. Calvin, J. Am. Chem. Soc., in press.

coefficient $\frac{k_{40}}{k_{30}}$ is 3.9, 3.2, and 3.0, respectively, at these pH's.

After certain difficulties of the procedure have been removed which make duplication of results difficult, the other members of the homologous series of trifluoroacetyl amino acids will be studied.

## CARBOXYDISMUTASE[1] IN PLANT CELLS

R. Clinton Fuller

As a result of kinetic and degradation studies, an enzyme capable of carrying out the reaction.

$$\underset{\text{(RuDP)}}{\text{ribulose diphosphate}} + CO_2 \longrightarrow 2\ \underset{\text{(PGA)}}{\text{phosphoglyceric acid}}$$

was implicated as the primary carboxylation reaction in photosynthetic organisms.[2] The existence of such a soluble enzyme in cell-free preparation was later demonstrated[3] and the enzyme was partially purified.[4,5] This report describes some observations designed to determine something about the intracellular distribution of this enzyme, particularly with reference to the photochemical apparatus (chloroplasts and fragments thereof).

Intact chloroplasts were obtained from spinach[6,7] by extraction with 2% NaCl (I) by resuspension in $H_2O$ and centrifugation at 35,000 rpm for 15 min, supernatant II, ppt III.

The distribution of enzyme in the various plant fractions was determined by measuring $C^{14}O_2$ fixation into PGA, using RuDP isolated from algae as substrate.[3] The results are shown in Table IV.

It appears that it is possible to separate the highly organized chloroplast of spinach from the rest of the cellular material in such a way as to have a significant fraction of the carboxydismutase associated with the chloroplast.

---

[1] This name has been suggested for the enzyme that catalyzes the reaction: ribulose diphosphate + $CO_2$ ⟶ 2 phosphoglyceric acid.

[2] J. A. Bassham, A. A. Benson, L. D. Kay, A. Z. Harris, A. T. Wilson, and M. Calvin, J. Am. Chem. Soc. 76, 1760 (1954).

[3] J. R. Quayle, R. C. Fuller, A. A. Benson, and M. Calvin, J. Am. Chem. Soc. 76, 3610 (1954).

[4] M. Calvin, R. Quayle, R. C. Fuller, J. Mayaudon, A. A. Benson, and J. A. Bassham, Fed. Proc. April, 1955, in press.

[5] E. Racker, Nature 175, 249 (1955).

[6] D. I. Arnon, P. R. Whatley, and M. B. Allen, J Am. Chem. Soc. 76, 6324 (1954).

[7] The author is indebted to Prof. Arnon, Dr. Allen, and Dr. Whatley, Department of Plant Nutrition, University of California, for performing the fractionation of the plant cells.

One washing with water, which also disorganizes the chloroplast, produces most of the enzyme in a soluble form free of the remaining chlorophyll-containing particles.

Table IV

Carbon-14-Labeled Compounds on the Chromatogram in Counts per Minute (10-min fixations of $C^{14}O_2$)

| | No substrate | Ribulose diphosphate | | | |
|---|---|---|---|---|---|
| Plant fraction* | Phospho-glyceric | Phospho-glyceric | Aspartic | Malic | Glutamic |
| I | 0 | 9,000 | -- | 400 | -- |
| II ($H_2O$ supernatant from I) | -- | 8,000 | -- | 200 | -- |
| III (green ppt. from II) | -- | 1,500 | -- | -- | -- |
| Broken chloroplasts and other particles from original I | -- | 500 | 200 | 50 | 100 |
| Plastid-free cell constituents from I | -- | 3,000 | 2,000 | 700 | -- |

*All fractions were diluted for use in the assay so that equivalent amounts of plant material based on a chlorophyll or wet-wt basis were used. Therefore, counts of PGA give a direct indication of distribution of the enzyme. The presence of any enzymes capable of acting on RuDP to produce substances other than PGA could only reduce the apparent carboxylation reaction in any fraction.

# FURTHER RELATIONS OF RESPIRATION TO THE QUANTUM REQUIREMENT IN PHOTOSYNTHESIS

James A. Bassham and Kazuo Shibata

In the previous two reports (UCRL-2709 and UCRL-2841, September 30, 1954 and January 10, 1955) a system was described for measuring the quantum requirement of photosynthesis and the respiration rate. It was found that with high light intensities, where photosynthesis greatly exceeds respiration (P/R = 12), the quantum requirement is 7.4, whereas at low light intensities (P/R = 1.4), the quantum requirement is 4.9 and appears to approach a value of 4.0 as P/R approaches zero. It was suggested that the lower requirement at small values of P/R is due to a contribution of energy from respiration to photosynthesis, in the form of adenosine triphosphate (ATP), which becomes more important as respiration rate becomes comparable with photosynthetic rate.

Analysis of the measured respiration rates obtained during twenty-minute periods in the dark following twenty minutes of photosynthesis at various light intensities shows a relation between dark respiration rate and previous rates of light absorption that is shown in Fig. 13. It will be seen that dark respiration rate increases with increasing amount of light absorption during previous photosynthesis. The value of $R_o$, the respiration rate after a long period of darkness, is obtained from Fig. 14, in which rates of oxygen evolution, corrected and uncorrected for dark respiration, are plotted as a function of the rate of light absorption. The uncorrected rate points fall on a very good straight line and the uncorrected rate extrapolated to zero gives the dark respiration rate of algae accustomed to a long period (several hours) of darkness. The assumption that the respiration rate is the same in a twenty-minute dark period following photosynthesis at a given level as during the period of photosynthesis seems justified by the experiments of Brown,[1] who used isotopic oxygen, $O^{18}$, to demonstrate that respiration rate of Chlorella was constant during alternate periods of light and dark (approximately twenty minutes) during experiments in which P/R ratio varied from 0.5 to 12. Brown's study also shows the long-term stimulation of the respiration rate in algae conditioned to periods of photosynthesis at a given level, compared with their respiration rates when conditioned by several hours' darkness.

The enhancement of respiration rate due to photosynthesis can be related to the contribution of energy from respiration to photosynthesis in the following way. The slope of the uncorrected oxygen-evolution curve in Fig. 14 corresponds to the reciprocal of the quantum requirement that would be found at very high light intensities if no light saturation could occur. This slope will be designated as $\phi_\infty$. The uncorrected $O_2$ evolution curve is then given by $G = \phi_\infty q - R_o$, where q is the number of quanta absorbed per second, $R_o$ is the dark respiration rate after a period of several hours' darkness, and G is the net number of molecules of oxygen evolved per second. The corrected rate of oxygen evolution is given by $P = \phi_q - R_o + R$, where R is the observed rate of respiration in molecules of oxygen absorbed per second.

The enhancement of respiration due to photosynthesis is given by $R - R_o$, whereas the number of quanta "saved" by the contribution of respiration energy

[1] A. H. Brown, Am. J. Bot. 40, 719 (1953).

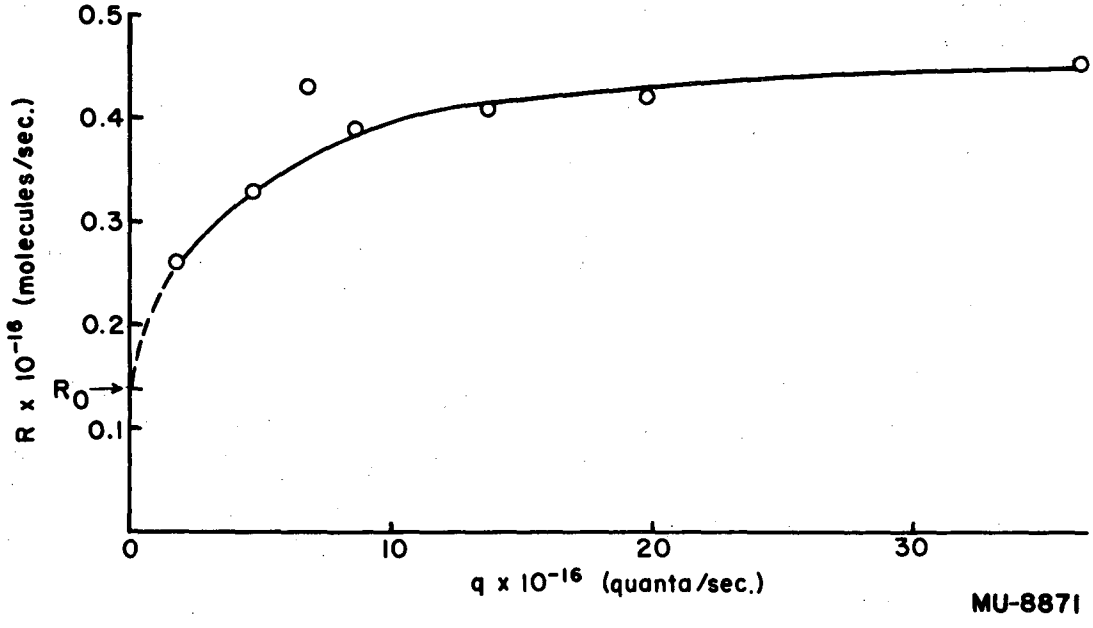


Fig. 13. Rate of oxygen absorption during respiration as a function of previous light-absorption rate.

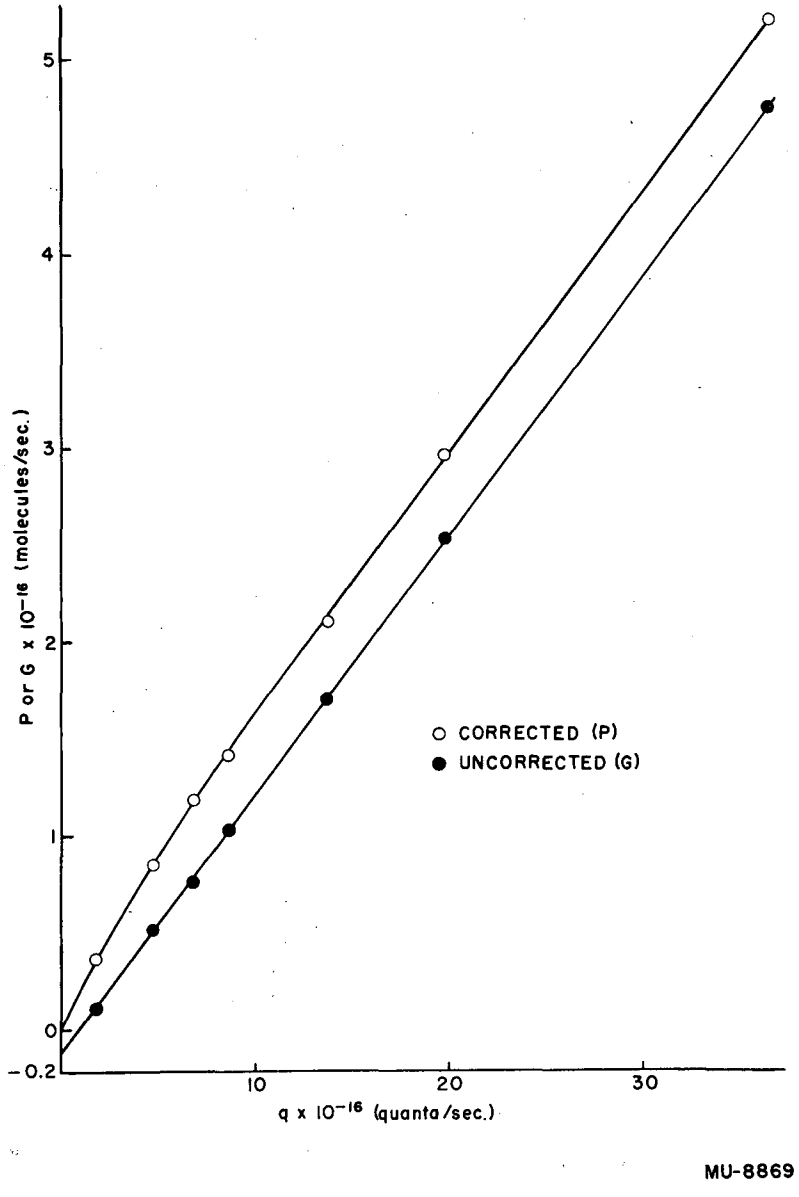


Fig. 14. Corrected and uncorrected rates of oxygen evolution during photosynthesis as a function of rate of light absorption.

to photosynthesis is just the difference between the actual quantum requirement and the quantum requirement at very intense light ($1/\phi - 1/\phi_\infty$) multiplied by the number of molecules of oxygen actually evolved during photosynthesis. This is

$$\begin{aligned} \Delta q &= P(1/\phi_\infty - 1/\phi) \\ &= P(1/\phi_\infty - q/P) \\ &= (P/\phi_\infty) - q. \end{aligned}$$

If $\Delta q$ is divided by the respiration enhancement, $R-R_o$, one obtains the number of quanta saved for each extra molecule of oxygen absorbed owing to enhanced respiration,

$$\frac{\Delta q}{R-R_o} = \frac{(P/\phi_\infty) - q}{R-R_o} .$$

But, it was found experimentally that

$$P = \phi_\infty q + R - R_o .$$

Therefore

$$\frac{\Delta q}{R-R_o} = \frac{1}{R-R_o} \quad \frac{\phi_\infty q + R-R_o}{\phi_\infty} - q ,$$

which reduces to

$$\frac{\Delta q}{R-R_o} = \frac{1}{\phi_\infty} .$$

This result, which is the consequence of the linearity of the G function in Fig. 14, means that, in this experiment, each extra molecule of oxygen absorbed by enhanced respiration results in the conservation of the same number of quanta as would be required for the evolution of a molecule of oxygen at a light intensity so high that the contribution of respiration to photosynthesis is negligible.

## METABOLISM OF THIOCTIC ACID IN ALGAE

R. Clinton Fuller and Hans Grisebach

Early observations on the biological activity of various compounds into which 6-thioctic acid (6T) is incorporated by algae indicated one that is more lipid-soluble than the thioctic acid. The major biologically active compounds found by chromatographic separation of such algal extracts were compounds that had $R_f$ values of 0.4, 0.7, and 0.9 in a solvent mixture of butanol-ethanol-$H_2O$. The origin showed biological activity that might be polymerized 6T.

The $R_f$ = 0.4 and $R_f$ = 0.7 components were identified as 6-thioctic acid and its sulfoxide, respectively. The compound at $R_f$ = 0.9 was not identified, and it was thought that it might be an artifact of the extraction procedure. The methods used were not sensitive enough to clarify further the status of this biologically active, thioctic-containing material.

The synthesis of thioctic-$S^{35}{}_2$ acid has made possible a further investigation of thioctic metabolism in algae and other organisms. The labeled 6T (83 μc/0.41 mg) was dissolved in 0.01 M phosphate buffer at pH 6.75. Scenedesmus was fed this solution at a concentration of 500 μg of 6T/gram of cells.

After various lengths of time, small samples of cell suspension were withdrawn and filtered rapidly, washed, and extracted with hot aqueous ethanol. The concentrated extracts were chromatographed in one dimension with either a mixture of butanol–0.5 N ammonia or butanol-ethanol-$H_2O$ (80:20:$H_2O$ to sat.). Five radioactive compounds were observed with the butanol-ammonia solvent, at the following $R_f$ values: 0.98, 0.51; 0.83, 0.17, and 0.1. The majority of the activity was observed at $R_f$ = 0.98, 0.51, and 0.17. The latter two spots were identified as 6T and 6T sulfoxide, respectively. In the butanol-ethanol-water solvent system both the 6T and 6T sulfoxide ran close to the solvent front, and at least seven different radioactive components could be observed.

The rate of metabolic uptake of the 6T by the algae in the dark is shown in Table V. In order to demonstrate that the compound observed on the front on the chromatograms was formed as a metabolic product of the cells and was not formed during the procedure, the 6T was chromatographed in the presence of an algae extract. The 6T solution was also added to an algae suspension and then the algae were killed immediately and extracted with ethanol. These solutions were then concentrated in the same manner as in the previous experiments and chromatographed. The distribution of the radioactivity in these controls and in a metabolic experiment is shown in Table VI. The substance on the front of the chromatogram appears to be a true metabolic product of the algae.

The thioctic-containing compound was eluted from the paper, hydrolyzed with 4 N HCl for 1 hour at 120°, and cochromatographed with unlabeled 6T. Two radioactive spots were formed as a result of the hydrolysis which corresponded to 6T and 6T sulfoxide, and the thioctic-containing compound was destroyed.

To get some information about the distribution of the compounds in the algae, the algae were fractionated. After 4 hours' contact of Chlorella with the 6T-$S^{35}{}_2$, the algae were filtered, washed two times with distilled water, suspended in water + phosphate buffer, and ruptured by 10-minute treatment in a 9-kc oscillator. Plastid material containing chlorophyll was isolated by ultracentrifugation. This plastid material was then extracted with hot 80% ethanol and the extract was chromatographed with butanol-0.5 N $NH_3$. Table VII shows the distribution of the radioactivity.

Because of the importance of 6T in the photosynthetic mechanism[1] it

[1] J. A. Barltrop, P. M. Hayes, and M. Calvin, J. Am. Chem. 76, 4348 (1954).

was of interest to study the metabolism of 6T in the light and the dark. 60 ml of a 0.5% algae suspension was kept under the usual conditions in the dark in the presence of 6T-$S^{35}_2$ for 4 hours. The algae were then filtered and washed two times with distilled water and resuspended in water + phosphate buffer. Half of this suspension was then kept in the dark for 10 minutes and the other half kept under light-saturated conditions. The amount of sulfoxide formed was 21% in the light and 19.5% in the dark; this difference is not significant.

Table V

Rate of Metabolic Uptake of the 6T by Algae in the Dark

| Time | % Uptake of 6-thioctic added |
|---|---|
| 1 min | 16% |
| 10 min | 24% |
| 30 min | 42% |
| 1 hour | 47% |

Table VI

Radioactivity Distribution

| Compound | dead algae extract + 6T | algae extracted + 6T | 5.25-hr uptake, dark |
|---|---|---|---|
| 6T | 79% | 85% | 6% |
| 6T-sulfoxide | 13% | 5% | 14% |
| Chromatogram front | 1.7% | 2.2% | 36% |

Table VII

Radioactivity Distribution

% of Total $S^{35}$ on Chromatogram

| Compound | Plastids | Supernatant |
|---|---|---|
| 6T | 7% | 15% |
| 6T-sulfoxide | 5% | 8% |
| Chromatogram front | 45% | 18% |

# DARK FIXATION OF $CO_2$ BY EUGLENA

E. Malcolm Thain and R. Clinton Fuller

The work on the dark fixation of $C^{14}O_2$ by Euglena has been continued. Degradations of the phosphoglyceric acid from two types of organisms have been completed. These vary only in the medium in which they have been grown. Subsequent treatment, and dark fixation methods (40 min) were identical. In the first case, the usual organic medium for Euglena was used; it contains acetate and a tryptic digest of casein. Organisms grown in this medium we designated "organic." In the second, an entirely inorganic medium was used, yielding "inorganic" Euglena.

It has been found that the dark and photosynthetic fixation patterns are somewhat different for these two types. This matter is under further investigation. It is of interest to note here, however, that in 40 min dark fixation, the organic Euglena extracts contain 2% to 7% PGA, while the inorganic Euglena contains 20% to 30% PGA. Both these samples have a similar pattern of radioactivity distribution in the carbon atom of PGA. (See Table VIII)

As was stated in the previous quarterly report (UCRL-2841, January 10, 1955), it was hoped that evidence would be found for the functioning of the photosynthetic cycle in the dark in Euglena. This was thought probable because of the high labeling of sugar phosphates in dark fixation.[1] The action of the cycle would be demonstrated by labeling in Positions 2 and 3 of glyceric acid.[2] The slight labeling that has been found might be taken as an indication that this cycle is operating slowly.

The other mechanism for the fixation of $C^{14}O_2$ is by the malic and fumaric enzyme systems, which can lead to carboxyl-labeled pyruvic acid and thus to carboxyl-labeled glyceric acid. If this compound can then be reduced to triose the scheme of sugar rearrangements shown in Fig. 15 can also lead to labeling in Positions 2 and 3 of a three-carbon fragment. These rearrangements depend on the reversal of some of the steps in the photosynthetic and pentose cycles, and they might be expected to take place during long periods when the organism is not photosynthesizing rapidly. These are the conditions of the dark fixation.

In summary, the slight labeling that has been found in Positions 2 and 3 of phosphoglyceric acid might be due to either the slow action of the photosynthetic cycle or to fixation by the "malic enzyme" route followed by reduction and sugar rearrangements.

---

[1] V. Lynch and M. Calvin, Ann. N. Y. Acad. Sci. 56, 890 (1953).
[2] J. A. Bassham, A. A. Benson, L. D. Kay, A. Z. Harris, A. T. Wilson, and M. Calvin, J. Am. Chem. Soc. 76, 1760 (1954).

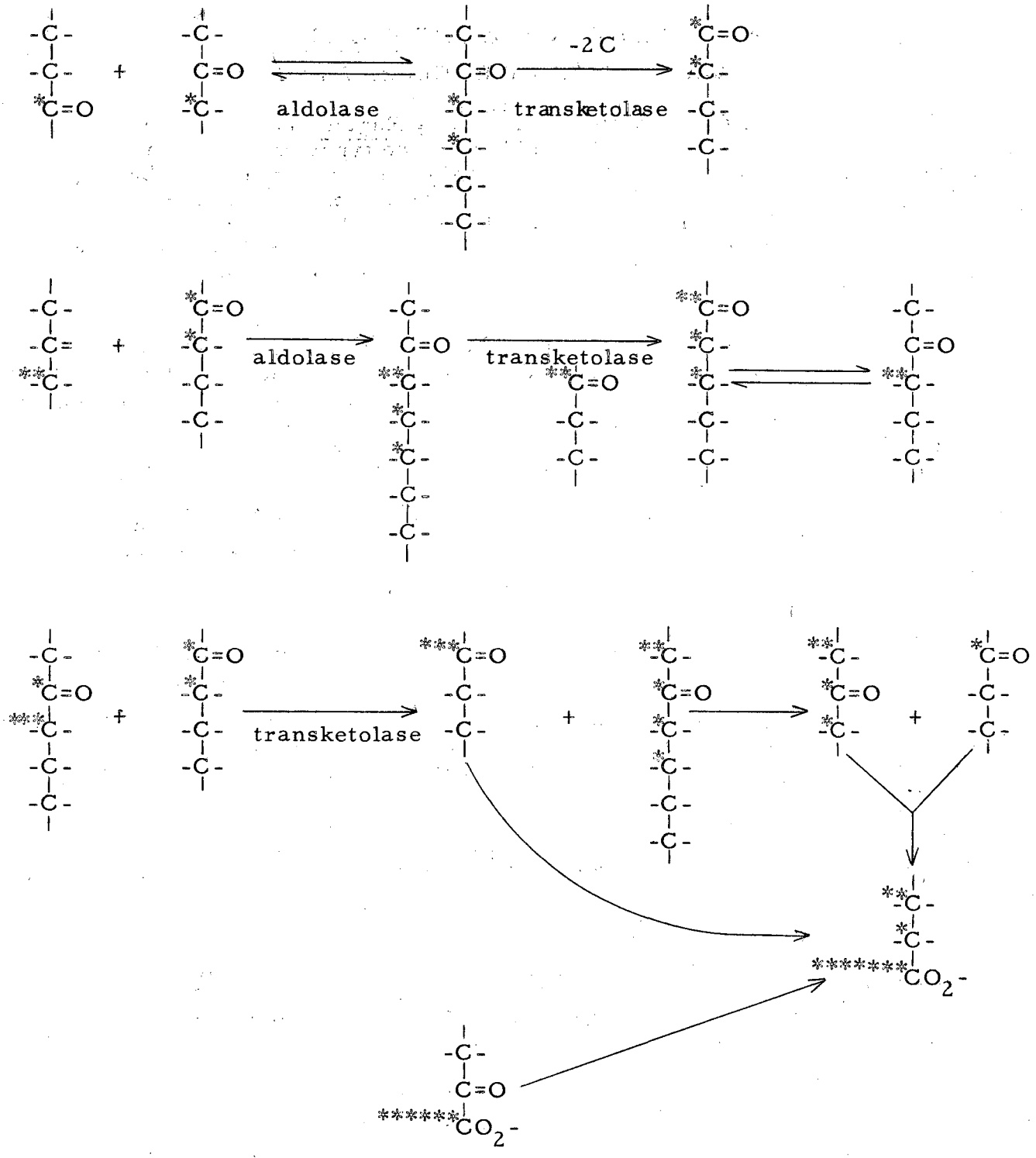


Fig. 15

Calvin

Table VIII

Percent Distribution of Radioactivity in PGA

| Glyceric Acid | 1 COOH | 2 -CHOH- | 3 $-CH_2OH$ |
|---|---|---|---|
| "Organic" | 94% | 1* | 2 |
| "Inorganic" | 95% | 1* | 3 |

*Standard error ± 0.3%, therefore carbon atom 2 = 0.7% to 1.3%.

## PREPARATION OF RIBULOSE DIPHOSPHATE

J. R. Quayle

During the past three months, work has been directed towards the preparation of ribulose-1,5-diphosphate (RuDP).[1] The method consists of the preparation of an enzyme system from spinach which can mediate the transformation of ribulose-5-phosphate to RuDP in the presence of adenoisine triphosphate (ATP).

After some initial difficulties with the preparation of the enzyme extract, the method is now working satisfactorily and is yielding RuDP in quantities of ca 30 mg per experiment. The purity of the product has been examined by enzymatic and HCl-hydrolytic dephosphorylation, and the resulting free sugars have been analyzed chromatographically and spectrophotometrically, using an orcinol test.[2] It appears that the product, obtained in the form of a barium salt, contains 31% by weight of pentose diphosphate. The pentose content liberated on dephosphorylation is a mixture of ribulose:ribose in the proportion of 70:30, and thus the RuDP must be contaminated with 30% of ribose diphosphate, presumably the -1,5-diphosphate (RDP), probably arising from the presence of a phosphoribokinase enzyme in the enzyme extract.

It seems likely that separation of these two diphosphates can be achieved by ion-exchange methods involving borate complexing. The ribofuranose diphosphate (assuming it to be the 1,5-diphosphate) should complex strongly with borate, whereas the straight-chain ribulose-1,5-diphosphate should not form a complex. We intend to prepare ca 100 mg of the pentose diphosphate mixture from several separate experiments, and then to separate the RDP from the combined yield. We hope by this means to obtain pure RuDP for further experiments.

---

[1] A. Weissbach, P. Z. Smyrniotis, and B. L. Horecker, J. Am. Chem. Soc. 76, 5572 (1954).

[2] B. L. Horecker, P. Z. Smyrniotis, and Hans Klenow, J. Biol. Chem. 205, 661 (1953).

Calvin

# INCORPORATION OF CARBON-14 IN PLANT PROTEINS

Ning Pon

Numerous investigations on the path of carbon in photosynthesis have been carried out, but few studies have been made on the role of carbon in the growth of proteins in plants. This study is concerned with the incorporation of $C^{14}O_2$ into a specific protein of Chlorella pyrenoidosa, namely, carboxydismutase. This protein was selected for study because (a) it can be separated from the plant cells without too much denaturation, (b) its biological activity can be used for following the course of the protein in purification and kinetic experiments.

The preparation of protein fractions from Chlorella is similar to standard procedures for obtaining proteins from other sources. There are three main steps: rupturing of the cells, solubilization of the protein, and fractionation. The rupturing of the cells and the subsequent solubilization (including the stabilization) of the proteins were done in one step. In this case the cells were sonicated after a 40-minute photosynthesis period in $C^{14}O_2$ in 0.05 M phosphate buffer pH 6.8. The whole cells and cell-wall components were separated from the protein and sugar solution by centrifugation, and the supernatant was used for the fractionation procedure.

Fractionation was accomplished by the use of ammonium sulfate. $(NH_4)_2SO_4$ was added to the supernatant until it was 30% saturated. The precipitate formed was centrifuged, redissolved in water, and dialyzed against $10^{-4}$ M potassium acetate solution. The 30% $(NH_4)_2SO_4$ supernatant was then made up to 40% (i.e., more salt was added) and the precipitate was collected and treated similarly. The 40% $(NH_4)_2SO_4$ was made up to 90%, which precipitated all the remaining water-soluble proteins.

The different fractions are denoted as follows: Fraction A, 0–30% saturated $(NH_4)_2SO_4$ fraction; Fraction B, 30–40% saturated; Fraction C, 40–90% saturated; and Fraction D, supernatant (protein-free). Each of these fractions has been subjected to some preliminary studies. The distribution of radioactivity is in fraction A, 0.7%; B, 0.7%; C, 4.3%; D, 94.2%. Using fraction B as a crude enzyme preparation with $NaHC^{14}O_3$ and unlabeled ribulose diphosphate as substrate, a specific biological activity was obtained, namely, paper chromatography showed only phosphoglyceric acid was formed.

The radioactive amino acids of fractions A and B were qualitatively determined by treatment of these protein fractions with 6 N HCl (100°C for 24 hours) and by subsequent two-dimensional paper chromatography using butanol-acetic acid and phenol-m-cresol- pH 9.3 borate buffer as developer. On the acid hydrolysis of these fractions, approximately 30% of the initial radioactivity was lost. Radioactive amino acids found in both fractions A and B are (in decreasing order or radioactivity): alanine, serine + glycine, valine, tyrosine, phenylalanine, leucine + isoleucine, glutamic acid, and aspartic acid.

The percent distribution of radioactivity in fraction A has been studied assuming the total radioactivity is equal to the sum of all the radioactive spots: alanine, 31%; serine + glycine, 19.2%; valine, 6.4%; tyrosine, 5.3%; phenylalanine, 5.1%; leucine + isoleucine, 4.8%; glutamic acid, 4.7%; aspartic acid, 3.3%. The rest of the radioactivity is in trace amino acids and nonamino acid

spots, one of which has 8.3% of the total radioactivity.

It is hoped that a relatively pure fraction, corresponding to carboxydismutase, can be obtained. This protein can then be subjected to ultracentrifugation, electrophoresis, and other physical chemical studies. In turn, kinetic studies can be made of the rate of incorporation of $C^{14}O_2$ into this protein, and--perhaps with the use of specific enzyme inhibitors--the role of carbon in the growth of the protein can be elucidated.

## A SCINTILLATION COUNTER FOR PAPER CHROMATOGRAMS

Kjell Steenberg and Andrew A. Benson

The purpose of the work was to develop a scintillation counter for counting $C^{14}$ activity on paper chromatograms. A photomultiplier tube and a preamplifier are mounted inside a metal cylinder. A lid with an opening equal to the window of the photo tube is screwed onto the end of the tube holder. The lid is made thin so as to get the counter as close to the paper as possible. This end of the counter is set directly on the paper. Provisions are made to prevent light from the top of the tube holder from reaching the window. To decrease light reflection between phosphor and tube window, we have applied silicone grease. The phosphor used is polystyrene with terphenyl as scintillation material. The emission spectrum for scintillations is in the range 3,750-4,800 Å, with $\lambda_p$ = 4,150 Å. Several Du Mont photomultiplier tubes were tested: Nos. 6292, 6342, 6217 (all 2 inches), and 6363 (3 inches). Of these, the 6292 tube was found to be the best with the phosphor used. Wave length at maximum response of the photocathode is 4,300-5,300 Å, $\lambda_p$ = 4,800 Å.

The light-absorption curve for the phosphor was found to correspond fairly well to the scintillation spectrum and the photocathode response. To find the best phosphor thickness, considering counting efficiency and background counts, we tried different thicknesses: 1, 2, 3, 5, 10, and ~100 mils. The counting efficiency for $C^{14}$ was found to be the same for the six thin ones and a little less with the 100-mil phosphor. The smaller efficiency with the last one is probably due to some light absorption in the phosphor. The background counting rate, however, seemed to decrease with decreasing phosphor thickness. The 1-mil scintillator, therefore, was chosen. The maximum range of $C^{14}$ betas in the phosphor material is about 8 mils, 1 mil absorbs about 75% of the betas.

To see if a reflection of light from the outer surface of the phosphor would give any increase in counting efficiency, a thin aluminum coat was evaporated onto the phosphor. It was given three opaque layers ( ~0.3 μ). No increase in efficiency was gained, but rather a small reduction due to the absorption of betas in the coating was observed. The same result was found with a 0.25-mil-thick aluminum sheet as reflector. That a reflection layer on the outside of the phosphor does not increase the counting efficiency is probably because there is already enough light produced in the phosphor by each β-particle to be detected by the counter.

An advantage of the aluminum coat in the phosphor would be to prevent the room light from getting into the tube. The coat would have to be so thick, however, that it would give appreciable β-absorption, as there were many small pinholes in any given single coat. We found that with the tube standing on the paper on a flat surface, no light from outside would come through to the tube. To spare the tube from fatique effects due to room light when the tube is moved from one spot to another on the paper, the high voltage of the scaler is switched off before the tube is moved. To facilitate the handling of the counter, it is operated with a counterweight over a pulley. The counting rate for this scintillation counter under proper voltage and discrimination was about 70% to 80% higher than with the Scott G. M. tube on the same $C^{14}$ spot. The background was about half of that of the Scott tube.

The uniformity of the counting area of the scintillation counter was found to be fairly good. A decrease in counting efficiency near the edge is probably due to a lower efficiency in the light collection from this area.

Coincident counter test

At low discrimination setting most of the background counts are due to noise (thermal electrons) in the phototube. As the electron emission from the photosurface is random, it should be possible to get rid of this type of background by a coincidence counter arrangement. We designed and tried an arrangement consisting of an aluminum block in which are bored two holes at right angles. Cylinders like the one used for the phototube in the first experiment are screwed into these holes. Two phototubes are set in the cylinders on a lucite prism inside the aluminum block, and bonded with silicone grease. The elliptical bottom of the prism is coated with one of the thin sheets of phosphor. Lucite was found to absorb very little light in the spectral range of the terphenyl scintillations. The parts of lucite block that are not covered by the phototube windows or the elliptic counting area on the bottom are covered with light-reflecting foils.

From the two preamplifiers the pulses go to two linear amplifiers, further to two discriminator circuits, and then to a coincidence circuit. The resolving time of this circuit is 2 μsec.

We found that this coincidence counter arrangement did not have any advantage compared to the single-tube counter. This is probably due to the decrease in optical geometry, and there may be some light absorption in the lucite block; the increase in tube voltage possible in the coincidence circuit was not enough to compensate for these losses. A coincidence circuit with a much shorter resolving time would decrease the number of background coincidences, but with the present arrangement the coincidence counter gives a lower counting efficiency at a higher background rate than does the single-tube scintillator counter.

# THE TERNARY SYSTEM n-PROPYL ALCOHOL, TOLUENE, AND WATER AT 25°

Elton M. Baker

The purpose of this study is to obtain a practical and completely miscible mixture of liquids for use as a scintillation solvent at a temperature of -14°C. The use of liquid scintillators for the determination of small amounts of radioactive tritium in water is at present not satisfactory because of the very low solubility of water in toluene. An aromatic solvent such as toluene is necessary, since aromatic solvents are the more efficient solvents for phosphors used in scintillation counting. Because water is almost completely insoluble in toluene it is necessary to use an additional solvent, such as an alcohol, to increase the solubility of water in the toluene. Other workers have used methanol and ethanol, obtaining counting efficiencies of 2% or less. It was believed that a mixture using n-propyl alcohol, which has a higher dielectric constant and greater hydrogen-bonding character than methanol or ethanol, might be useful for counting tritium as water, for this mixture could contain a higher weight percent of toluene and--with less quenching of the energy-transfer process by the alcohol--should have greater counting efficiency.

This study of the ternary system, toluene--n-propyl alcohol--water, has been carried out at 25°C. The n-propyl alcohol was purified by distillation; only the middle fraction was used. It had a specific gravity of 0.7999 and index of refraction of 1.3854 at 25°C. The toluene was distilled over sodium by the same procedure and gave a specific gravity of 0.8593 and a refractive index of 1.4921 at 25°C. Water was redistilled from potassium permanganate and sodium hydroxide solution. Its specific gravity of 0.99707 and index of refraction of 1.3325 were used as standards to obtain the values for the other liquids. A 10-ml pycnometer was used to determine the specific gravity and an Abbé refractometer was used to determine refractive indices. A constant-temperature bath at 25.0 ± 0.1°C was used to control the temperatures of all liquids.

The n-propyl alcohol and toluene were weighed into ground-glass-stoppered flasks and brought to 25°C in the constant-temperature bath. Then water was added in small quantities, from a calibrated burette with shaking; the temperature of the solution was allowed to return to 25°C before further additions of water. When the end point was reached, a milky translucent mixture that remained permanent for 30 minutes, the refractive index and specific gravity were determined. From these data, a graph was plotted of the weight percent of alcohol corresponding to a definite refractive index of the water-saturated ternary mixture. This graph was used to determine the percent of alcohol in equilibrium mixtures of two phases, water and toluene, each containing n-propyl alcohol.

From a plot on an equilateral triangular diagram of data in Table IX, one may choose the best mixture to give the largest quantity of toluene containing the necessary amount of tritiated water with the minimum of alcohol at 25°C. The solubilities of the toluene-alcohol-water system are also being measured at -14°C, but are only partly completed; the studies will be continued with further work on other aliphatic alcohols and aromatic solvents to obtain a comparison of the counting efficiency as well as of the effect of alcohols on the quenching of the energy-transfer process in scintillation mixtures in which the actual activity remains constant.

Calvin

Table IX

Mutual Solubilities for the Ternary System,
Toluene–n-propyl Alcohol–Water at 25°C

| Weight % Toluene | Weight % n-Propyl Alcohol | Refractive Index | Specific Gravity |
|---|---|---|---|
| 91.016 | 8.493 | 1.4815 | 0.8537 |
| 88.978 | 10.297 | 1.4789 | 0.8530 |
| 85.784 | 13.190 | 1.4750 | 0.8516 |
| 79.913 | 18.300 | 1.4672 | 0.8493 |
| 71.136 | 25.906 | 1.4572 | 0.8468 |
| 65.742 | 30.104 | 1.4518 | 0.8455 |
| 58.484 | 36.001 | 1.4431 | 0.8446 |
| 47.442 | 44.089 | 1.4322 | 0.8441 |
| 41.460 | 47.820 | 1.4238 | 0.8450 |
| 29.663 | 54.526 | 1.4091 | 0.8494 |
| 18.299 | 56.596 | 1.3938 | 0.8536 |
| 11.697 | 53.954 | 1.3829 | 0.8773 |
| 4.573 | 42.525 | 1.3684 | 0.9128 |
| 1.855 | 30.295 | 1.3578 | 0.9420 |
| 0.609 | 22.653 | 1.3519 | 0.9601 |
| 0.444 | 20.969 | 1.3505 | 0.9637 |

# MYLAR FILM WINDOWS FOR SCOTT TUBES

Paul M. Hayes

The Scott tube, an atmospheric-pressure, large-window Geiger tube, has long been in use by the Bio-Organic Group for counting the low-level beta radiation of $C^{14}$. It has worked very well but is extremely fragile, since it has a thin mica window covering the end of the tube with an opening about 60 mm in diameter. This mica easily breaks on any sudden change of pressure, and a better window covering would be a decided advantage.

Very thin, yet very strong, plastic films of "Mylar," polyethylene terphthalate available from DuPont, provide the type of material needed to replace the mica. An initial attempt of simply replacing the mica with Mylar failed. After the Mylar window was sealed the tube was thoroughly flushed with "Q" gas (Nuclear, Chicago) and the stopcock at the top of the tube was closed. The tube worked very well at first, but after a short time the threshold voltage would rise and the plateau would vanish. Air rapidly diffused into the tube through minute pinholes in the film. Since almost every thin plastic sheet would probably contain pinholes, we have solved this problem by redesigning the tube. Provision is made to have a continuous sweep of quench gas in order to keep a slight positive pressure on the inner side of the film.

The film we are using at present has a thickness of 0.00025 inch, which gives a density of about 1 $mg/cm^2$. With this film we now have a counting efficiency of 20%, as against an efficiency of about 14% with the mica-window tubes. "Mylar" film G-M tubes thus offer the advantages of both greater strength and greater efficiency than tubes with mica end windows.

Calvin

# NUCLEAR CHEMISTRY

Glenn T. Seaborg and Isadore Perlman in charge

## NUCLEAR REACTION MECHANISMS: FISSION-SPALLATION COMPETITION IN HEAVY ELEMENTS

### Group Program and Cross Sections for Reactions of $Pu^{239}$, $Pu^{238}$, and $Pu^{242}$ with Alpha Particles

Richard A. Glass, Robert J. Carr,
James W. Cobble, and Glenn T. Seaborg

### Program

The program in progress for two years[1], for determining cross sections and excitation functions for reactions of heavy-element nuclei with alpha particles and deuterons (in the low-energy range), has been continued and expanded. Cross sections measured include those for (α, f), (α, pxn), (α, xn), and (α, 2pxn) reactions, and (d, f), (d, xn) and (d, pxn) reactions, where x is always less than six. From extensive data on this limited number of simple reactions, to be collected over the next few years, fruitful theoretical interpretations are anticipated. Past, present, and future plans are reviewed in this report.

There are three aspects of interest in the program. (a) The determination and interpretation of the absolute fission and spallation cross sections is the primary objective. (b) The clarification and--in some cases--determination of decay properties is essential to the primary objective, and interesting in its own right. (c) The determination of optimum bombardment conditions for production of specific isotopes in future work is a valuable secondary result.

### Experimental Procedures

The character of the experimental procedures is largely governed by the rarity and intense alpha-radioactivity of many of the target nuclides. The radioactivity necessitates that chemical operations be carried out in gloved boxes and that extreme caution be exercised. Partly because of these problems, stacked-foil and recoil techniques are presently unfeasible.

The experimental procedures leading to the calculation of the absolute cross sections can be reviewed briefly. (a) Milligram amounts of target isotopes ranging in atomic number from 88 (radium) through 96 (curium) are irradiated (bombarded) in the Crocker Radiation Laboratory 60-inch cyclotron. About ten bombardments with alpha particles (spaced 3 Mev apart in alpha-particle energy) cover the 19-to-47-Mev range, which extends from the heavy-element potential barrier for alpha particles to the upper limit of the cyclotron. Six bombardments cover the corresponding range of 9 to 23 Mev for deuterons. (b) Total numbers of charged particles that have passed through the target are determined from Faraday cup measurements. (c) Densities of target atoms in uniformly electroplated target plates are measured by counting techniques and by weighing. (d) Product atoms formed in the bombardment

are separated successfully from the entire target solution by radiochemical procedures for fission-product and actinide elements. (e) Atoms of product isotopes formed are calculated from disintegration-rate measurements with geiger counters, alpha counters, windowless proportional counters, and the alpha-pulse analyzer. (f) From the preceding data, cross sections are determined with the formula

$$\sigma = \frac{\text{product atoms}}{\frac{\text{Target atoms}}{\text{cm}^2} \times \text{total beam particles}} = \frac{N}{\frac{n}{\text{cm}^2}(It)}$$

(g) Fission-yield curves are determined from the fission-product cross sections at each energy, and these are integrated to obtain total fission cross sections. (h) Total fission and individual spallation excitation functions summarize the results for each isotope. (i) Supplementary decay-scheme work is done where new information can be gained.

Interpretation of Data

Excitation functions for many isotopes, with both alpha particles and deuterons, must be gathered before any broad generalizations with regard to mechanisms of reaction can be made. Certain lines of thinking, however, mainly in terms of compound-nucleus effects, are useful as a working basis for the investigation. Observations and interpretations of interest are enumerated below. (a) Fission-yield curves at various energies for each target isotope are analyzed for the change from asymmetric to symmetric fission with increasing excitation energy. (b) The variation of fission-yield curves as well as fission excitation functions from one target isotope to the other is noted. (c) Spallation excitation functions for each target isotope are analyzed for reactions which survive the predominant fission reaction more successfully. Comparisons are made with data from lighter elements where small fission reactions (or the absence of them), as well as lower potential barriers, change the character of nuclear reactions. Quantities affecting relative cross sections include $Z^2/A$, odd-even character, level density, and nucleon binding energy of nuclides formed in the reaction. The effects of these quantities, in theory, operate on any nuclide resulting from evaporation of particles from the initial compound nucleus formed between target nucleus and bombarding particle, and may determine whether the de-excitation mode is fission, neutron emission, or gamma-ray emission. Non-compound nucleus effects, such as various stripping processes and complex-particle emission--e.g., tritium emission--are certainly operating and must be considered. (d) Spallation yields for specific reactions are compared between target nuclides. (e) Fission excitation functions are compared with spallation excitation functions for each target isotope for the specific purpose of analyzing the competition between these fundamentally different nuclear reactions. The comparison is extended to results from all isotopes. (f) The excitation function for the sum of all spallation and fission cross sections (total reaction cross section) is used to calculate a nuclear radius for the target nucleus. (g) Finally, basic mechanisms of nuclear reactions are suggested as far as possible.

Seaborg

## Cross Sections for Reactions of $Pu^{239}$ with Alpha Particles

The initial investigation of the program, by Glass, Cobble, and Seaborg,[1,2,3] yielded fission and spallation excitation functions for the (α, f), (α, n), (α, 2n), (α, 3n), (α, 4n), (α, 5n), (α, p), (α, p2n), (α, p3n) and (α, p34n) reactions in the range of alpha-particle energies from 19 to 47 Mev.

An isotope diagram is useful for picturing the isotopes involved in the series.

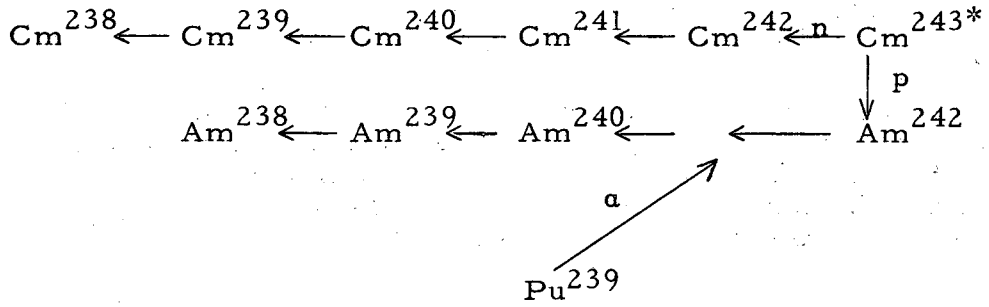


The preliminary results can be summarized briefly. (a) The fission-yield curves and excitation function were similar in the main features to those obtained with $U^{235}$,[4] and other heavy elements.[5,6] (b) The spallation excitation functions revealed, first, that the (α, n) cross section was rather small and constant between 1 and 2 millibarns. (c) The (α, 2n) reaction was surprisingly prominent as manifested by an excitation function rising to a peak above 13 millibarns at about 29 Mev. (d) The (α, 3n) and (α, p) excitation functions rose to low peaks of 3.5 and 1.5 millibarns respectively in the region of 36 Mev. (e) A surprisingly important (α, p2n) reaction indicated that when three particles are emitted from the compound nucleus, a proton is probably one of them. The excitation functions peaked at a value above 9 millibarns, again around 36 Mev. An (α, t) mechanism is possible for this reaction. (f) The (α, 4n), (α, 5n), (α, p3n), and (α, p4n) cross sections were below 1 millibarn (with the possible exception of the (α, p4n) cross sections) and rising in the region from 38 to 47 Mev.

## Cross Sections for Reactions of $Pu^{238}$ and $Pu^{242}$ with Alpha Particles

The second investigation, this time by Carr, Cobble, and Seaborg (1954),[3] yielded excitation functions for the (α, f), (α, n), (α, 2n), (α, 3n), and (α, 4n) reactions of $Pu^{238}$ and the (α, 2n) and (α, 4n) reactions of $Pu^{242}$. These data, with the results from $Pu^{239}$, give the variation of cross sections with A at constant Z (mass effect) for a number of reactions.

Isotope diagrams are given below.

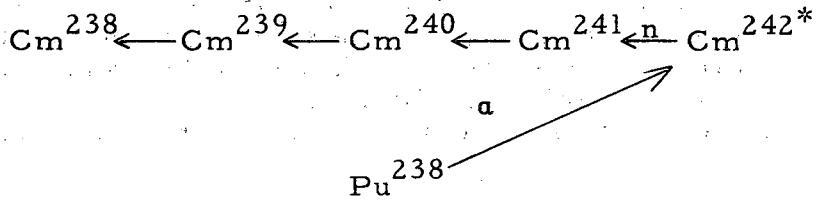


Seaborg

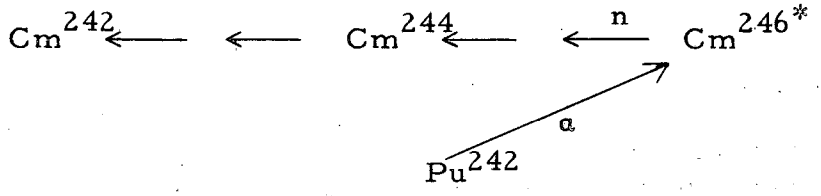


The spallation excitation functions for $Pu^{238}$ furnish interesting points of comparison with the (α, n) and (α, 2n) reactions of $Pu^{239}$. (a) The (α, n) cross section is constant at 6 millibarns--much higher than the 1- to 2- millibarn values for $Pu^{239}$. (b) The (α, 2n) excitation function peaks at 24 Mev with a 14-millibarn cross section. The peak is the same magnitude as the corresponding $Pu^{239}$ peak, but occurs about 5 Mev lower in energy. The (α, 2n) and (α, n) excitation functions cross in the region of 40 Mev.

The (α, 2n) reaction is very prominent in $Pu^{242}$. The excitation function peaks about 100 millibarns below 24 Mev. Thus the (α, 2n) reaction is most prominent with the plutonium isotope of highest mass, and therefore lowest $Z^2/A$ value. The two even-even plutonium isotopes peak at the same energy, which is lower than that for the even-odd isotope $Pu^{239}$. This is one of the unpredictable features that only further information will clarify.

## Cross Sections for Reactions of $Pu^{239}$ with Deuterons

Walter M. Gibson, Richard A. Glass, James W. Cobble, and Glenn T. Seaborg

### Objectives

Excitation functions for the (d, f), (d, n), (d, 2n), (d, 3n) and (d, 4n) reactions of $Pu^{239}$, nearly completed, constitute the first deuteron data of the program. Interesting comparisons of shape and magnitude are promised between these results and the fission and spallation cross-section curves previously determined for the alpha-particle reactions of $Pu^{239}$. The nuclides $Am^{238}$, $Am^{239}$, and $Am^{240}$ from the (d, xn) and also (α, pxn) reactions of $Pu^{239}$ afford a direct comparison of alternative methods of isotope production. The compound nucleus, $Am^{241*}$, will also be formed in a later series of bombardments of $Np^{237}$ with alpha particles.

The isotope diagram shows the isotopes involved in this series.

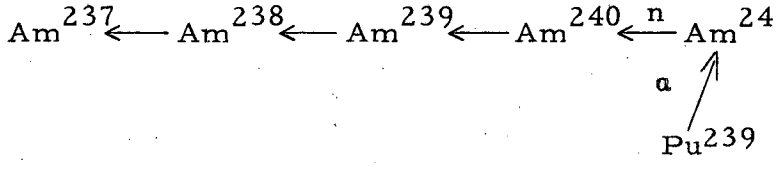


The plutonium isotopes produced by (d, pxn) reactions, possibly in high abundance, are undetectable with present techniques because of the intense alpha radioactivity of the target nuclide.

Seaborg

## Experimental Procedures

The 6-bombardment sequence includes deuteron energies of 10, 13, 16, 19, 21, and 23 Mev. Milligram amounts of $Pu^{239}$ with high isotopic purity are available for the experiments. Experimental methods are those used with the alpha-particle experiments, with the difference that no lactate elution from a cation exchange column is performed. An alcohol-HCl elution, following initial steps to remove Al (with NaOH) and plutonium (with an anion column), separates americium from the rare earths, which are precipitated with americium in $LaF_3$ carrier. Fission products separated are strontium, cadmium, and barium from all bombarded targets, and cerium, neodymium, europium, and terbium from three bombardments. Special problems with the electron-capturing nuclides, $Am^{238}$, $Am^{239}$, and $Am^{240}$, were solved by experiments for determining the counting efficiencies of these three nuclides in a windowless proportional counter. Alpha-emitting daughters from the decay of these nuclides were chemically separated and measured for this purpose.

## Results

Preliminary cross-section results for two bombardments are tabulated below.

| Deuteron Energy | Total Beam | Amount of Plutonium | $\sigma$ (d, n) | $\sigma$ (d, 2n) |
|---|---|---|---|---|
| 9 Mev | 13.9 μah | 0.412 mg | 1.2 mb | 10.6 mb |
| 13 Mev | 20.0 μah | 0.249 mg | 10.4 mb | 91.5 mb |

The sharp rise in (d, n) cross section between 9 and 13 Mev is interesting. Since the (α, n) cross section for $Pu^{239}$ is essentially constant with increasing bombardment energy, a flat (d, n) excitation function was expected, because a stripping-type process is much more likely for this latter reaction. Further spallation cross sections and the fission results are in the process of calculation.

Supplementary decay-scheme information resulted from an irradiation of 11.7 milligrams of $Pu^{239}$ with 30 microampere hours (total beam) of 17-Mev deuterons. Windowless proportional counter efficiencies for the electron-capture disintegration of $Am^{238}$, $Am^{239}$, and $Am^{240}$ were determined from counting-rate decay curves on this instrument, and from the absolute disintegration rates as calculated from the alpha-decaying plutonium daughters, which were periodically extracted from the americium. Efficiencies were 8.9 percent and 8.0 percent (2 separate plutonium extractions) for $Am^{238}$; 15.7 percent for $Am^{239}$, and 91.1 percent for $Am^{240}$. The very low $Am^{238}$ and $Am^{239}$ efficiencies necessitate a repeat experiment for confirmation. With the electron-capture disintegration rate of $Am^{239}$, an alpha branching ratio of $4.1 \times 10^{-5}$ and partial alpha half life of 33 years were calculated for this isotope. Finally, the absence of $Cm^{240}$ in the americium sample permitted lowering the upper limit for negatron branching of $Am^{240}$ to the value $1.4 \times 10^{-8}$.

## Cross Sections for Reactions of $Pu^{240}$ with Deuterons

E. Victor Luoma, Richard A. Glass, and Glenn T. Seaborg

Excitation-function determinations for the (d, f), (d, 2n), (d, 3n), and (d, 4n) reactions of $Pu^{240}$ are planned. The effect of mass of the target isotope (mass effect) on cross section for deuterons between $Pu^{240}$ and the previous investigated $Pu^{239}$ is of primary interest in this sequence. The mass effect for both deuterons and alpha particles among plutonium isotopes will then be defined, and one important phase of the program concluded.

An isotope diagram for this series is given below.

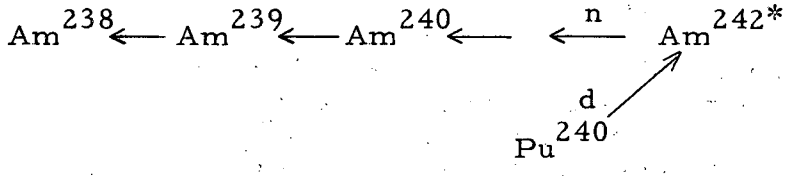


The isotopic composition of the $Pu^{240}$ available is tabulated below.

| Isotope | Abundance |
|---|---|
| $Pu^{239}$ | 12.20% |
| $Pu^{240}$ | 87.172% |
| $Pu^{241}$ | 0.583% |
| $Pu^{242}$ | 0.044% |

From this, it is seen that the growth of $Am^{241}$ alpha activity from the $Pu^{241}$ constitutes an inherent difficulty. Experimental procedures are those used for the $Pu^{239}$ bombardments.

## Cross Sections for Reactions of $U^{233}$ with Alpha Particles

T. Darrah Thomas, Richard A. Glass, and Glenn T. Seaborg

### Objectives

Excitation functions for the (α, f), (α, n), (α, 2n), (α, 3n), (α, 4n), (α, 5n), (α, p), (α, pn), (α, 2pn), (α, p3n), and (α, p4n) reactions of $U^{233}$, when completed, will be the first investigation with other than a plutonium isotope. The uranium isotopes $U^{233, 234, 235, 236, 238}$ offer a sequence of available isotopes complementary to the plutonium isotopes, $Pu^{238-242}$. A slightly decreased fissionability for the uranium isotopes is anticipated, but its determination must await further data. Since $U^{233}$ is analogous to $Pu^{239}$ in nuclear type and proximity to maximum beta stability, variations in cross sections due solely to the change in atomic number (change effect) should be apparent.

The isotope diagram for the sequence is as follows:

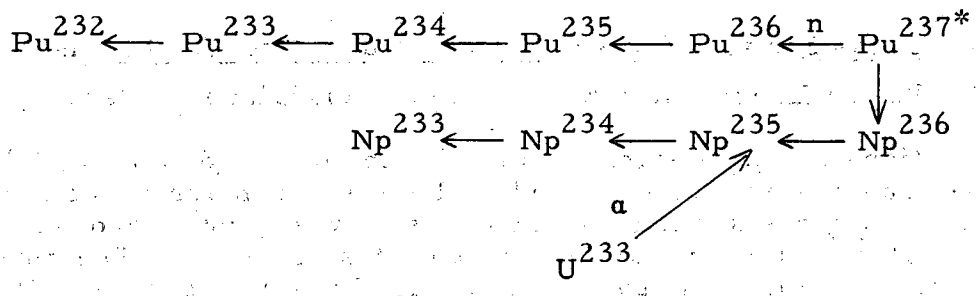


The undiscovered isotope, $Pu^{233}$, should be characterized in the course of the bombardments.

Experimental Procedures

The isotopic purity of the uranium is 97 percent $U^{233}$. The series consists of ten alpha-particle bombardments at 19, 22, 25, 28, 31, 34, 37, 40, 43, and 46 Mev. The fission products zirconium, cadmium, and cerium and occasionally neodymium, europium, and terbium are isolated by standard chemical procedures. The spallation products, plutonium and neptunium, are separated from the uranium, by coprecipitation of their fluorides with $LaF_3$. Anion-column separations with concentrated and dilute HCl, alternately containing oxidizing and reducing agents, and an extraction with TTA finally yield pure plutonium and pure neptunium. Because of the short half lives of some of the plutonium isotopes speed is essential. The other experimental techniques are similar to those used with the plutonium bombardments.

Results

Preliminary cross sections for (α, n) reaction are tabulated below.

| Alpha-Particle Energy (Mev) | (α, n) Cross Section ($Pu^{236}$) (mb) |
|---|---|
| 20 | 0.27 |
| 23 | 0.22 |
| 26.2 | 0.063 |
| 27.9 | 0.27 |
| ~44 | 0.28 |

The (α, n) cross section, with the exception of the questionable 26.2-Mev value, is constant with increasing energy, as was this cross section for $Pu^{239}$ and $Pu^{238}$. The low values for the cross section compared to $Pu^{239}$ and $Pu^{238}$ indicate that the supposed decreased fissionability of uranium does not favor a high (α, n) reaction. There is some indication that the (α, 3n) cross sections are fairly high. Perlman, Morgan, and O'Connor[7] determined values of 0.5 mb and 1 mb for the (α, n) and (α, 3n) reactions, respectively, at 44 Mev for $U^{233}$.

## Cross Sections for Reactions of $U^{235}$ with Alpha Particles

Robert Vandenbosch, Richard A. Glass, and Glenn T. Seaborg

There are three principal features of interest in this sequence. (a) The $U^{235}$, $U^{233}$, and $U^{238}$ results will serve to define the mass effect for uranium isotopes. The $U^{235}$ experiments, however, represent the first determination between two even-odd isotopes ($Pu^{238}$ and $Pu^{242}$ represented an even-even pair). (b) The radiochemical-fission excitation function can be checked with the fission-chamber curve for $U^{235}$. The copious fission results for this isotope render it a crossroads for intercomparing data. (c) Taken with deuteron bombardments of $Np^{237}$, the investigation constitutes a study of the compound nucleus $Pu^{239*}$.

The isotopes to be determined are included in the following diagram.

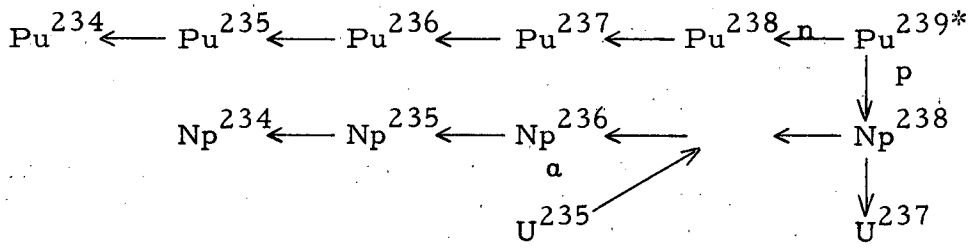


The uranium used is 99.94 percent $U^{235}$. The experimental procedures are similar to those used with $U^{233}$ with the exception that some target uranium is counted for $U^{237}$ produced by the (α, 2p) reaction.

## Cross Sections for Reactions of $U^{238}$ with Alpha Particles

Susanne E. Ritsema, Richard A. Glass, and Glenn T. Seaborg

The isotopes $U^{238}$ and $Th^{232}$ are experimentally good for the study of one-proton-out and two-proton-out reactions: (α, p), (α, pn), (α, p2n), (α, p3n), (α, 2p), (α, 2pn), and (α, 2p3n) reactions. Since a proposed explanation for the prominent (α, p2n) reaction of $Pu^{239}$ is tritium emission, this effect may characterize $U^{238}$ spallation. Complex particle emission may also determine (α, 2pn) and (α, 2p3n) product yields by (α, $He^3$) and (α, αn) mechanisms, respectively. Yield and Q-value considerations may help settle the question. The $U^{238}$ excitation functions will also serve to define the mass effect for uranium. Thirdly, the fission excitation function can be compared with Jungerman's fission-chamber results.[4] Finally, $U^{238}$ is isotonic with $Am^{241}$.

The following isotope diagram for this series shows the three spallation product elements for which yield data are being obtained.

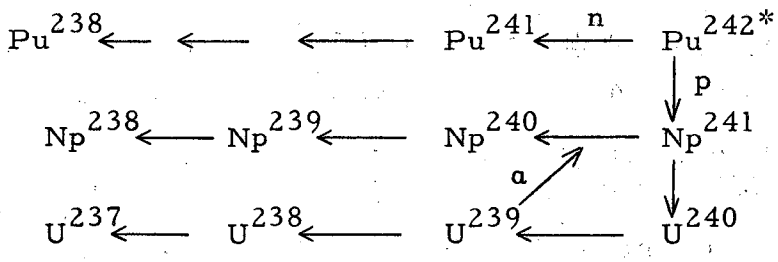


The uranium used is 99.9993 percent $U^{238}$. The experimental procedures employed are those used with $U^{235}$.

## Cross Sections for Reactions of $Am^{241}$ with Alpha Particles

Bruce M. Foreman, Richard A. Glass, and Glenn T. Seaborg

$Am^{241}$ is the highest-Z isotope studied. Eventually, excitation functions for other isotopes in this interesting heaviest-element region, such as $Am^{243}$, $Cm^{242}$, and $Cm^{244}$, will be determined.

The experimental procedures have been outlined on previous pages. The chief distinction of this series is the number of lactate elution columns necessary to separate americium, curium, and berkelium.

The isotope diagram for the sequence reveals the limited number of spallation products for which data can be obtained.

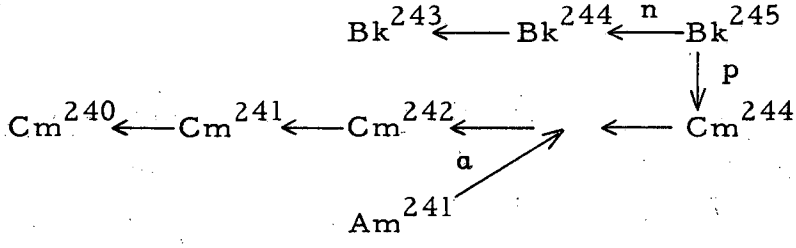


A preliminary cross section of 78 mb for the sum of the (α, n) and (α, 2n) reactions at 31 Mev was obtained from the first bombardment.

References

1. R. A. Glass, J. W. Cobble, and G. T. Seaborg, in Chemistry Division Quarterly Report, University of California Radiation Laboratory Report No. UCRL-2455 (January 11, 1954).

2. R. A. Glass, Studies in the Nuclear Chemistry of Plutonium, Americium, and Curium and the Masses of the Heaviest Elements, (Thesis), University of California Radiation Laboratory Report No. UCRL-2560 (June 1954).

3. R. A. Glass, R. J. Carr, J. W. Cobble, and G. T. Seaborg, Bull. Am. Phys. Soc. 29, No. 8, Abstract G8 (1954).

4. J. Jungerman, Phys. Rev. 79, 632 (1950).

5. A. S. Newton, Phys. Rev. 75, 17 (1949).

6. H. A. Tewes and R. A. James, Phys. Rev. 88, 860 (1952).

7. I. Perlman, P. R. O'Connor, and L. O. Morgan, United States Atomic Energy Commission Declassified Document AECD-2289 (Declassified September 10, 1948).

# DECAY CHARACTERISTICS OF SOME HEAVY ISOTOPES

Isadore Perlman, Frank Asaro, Frank S. Stephens,
John P. Hummel, and Richard C. Pilger

## $100^{254}$

Gamma rays of 41 kev (0.02%) and 96 kev (0.028%) were observed in coincidence with alpha particles. L x-rays were also observed in an abundance corresponding to an alpha decay to the first excited state of 15%.

## $99^{253}$

From alpha-particle spectrograph measurements, $99^{253}$ was found to have alpha groups of 6.642 Mev (~86%), 6.600 Mev (~9%), and 6.548 (~5%) Mev. Gamma radiations of 42 kev (0.1%), 54 kev (~0.03%), 112 kev (0.03%) and 393 kev (0.04%) were observed with scintillation and proportional counters. These correspond to a decay scheme shown below.

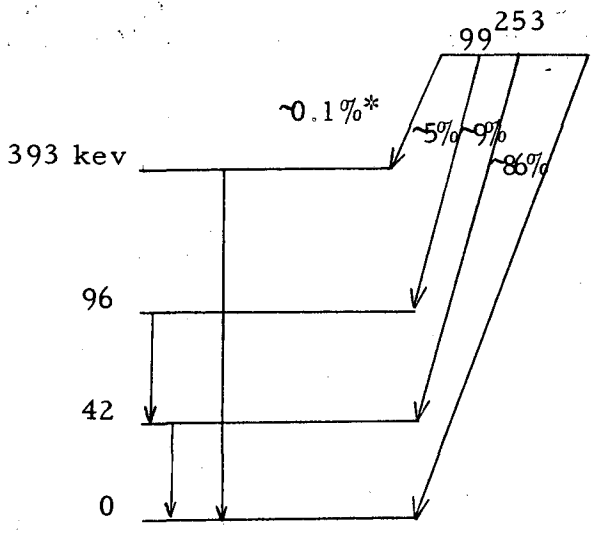


*Using an alpha-pulse analyzer, Albert Ghiorso observed an alpha group at 6.25 Mev in about 0.1% abundance.

## $Cf^{250,252}$

The alpha spectrum of $Cf^{250,252}$ was observed with an alpha-particle spectrograph. $Cf^{252}$ had alpha groups of 6.112 Mev (84.5%) and 6.069 Mev (15.5%). $Cf^{250}$ had alpha groups of 6.024 Mev (83%) and 5.980 Mev (17%).

L x-rays and gamma rays of 42 kev (0.014%) and 100 kev (0.00013%) were observed in coincidence with alpha particles.

$Cf^{249}$

Gamma rays of 395 kev (60%) and 340 kev (16%) were observed in coincidence with $Cf^{249}$ alpha particles. The 340-kev gamma ray was in abundant coincidence with L x-rays.

$Cm^{245}$

$Cm^{245}$ has gamma radiations of 101 kev (80%) and 173 kev (13%) in coincidence with alpha particles. The 101- and 173-kev radiations were not in high coincidence. The 101-kev radiation had a distorted shape with possible radiations at 118 kev ($K_\beta$ x-rays) and 134 kev. The gamma radiations are similar to those observed in $Cm^{243}$ decay.

$Cm^{244}$

The abundances of $\alpha_0$ and $\alpha_{43}$ in $Cm^{244}$ decay were measured with an alpha-particle spectrograph as 76.7% and 23.3% respectively. Their gamma-energy separation was 43.0 kev. A new alpha group, 142.7 kev lower in decay energy than the main group, was found in an abundance of 0.014% . The ratio of the energies of the second excited state to the first excited state is 3.32. From the Bohr-Mottelson theory, the 43- and 143-kev states have spins of 2+ and 4+. The conversion coefficient of the 43-kev gamma ray was measured and indicated the spin of the 43-kev state was 2+.

$Cm^{243}$

The 277-kev gamma ray was found to be in coincidence with a 100-kev gamma ray. The abundance of the coincidences was 1.8% of the 277-kev gamma ray. Since the maximum alpha population of the state dropping this 100-kev gamma ray is 2%, the 100-kev transition must have electric dipole multipole order, from conversion-coefficient considerations.

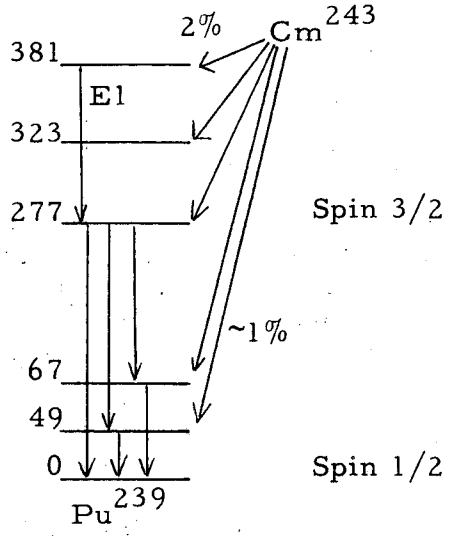


Seaborg

The conversion coefficient of the 277-kev radiation indicates a mixture of dipole and quadrupole radiations. Since the spin of the $Pu^{239}$ ground state is known to be 1/2, the spin of the 277-kev state is then 3/2. The 381-kev state, which is populated by ~2% alpha emission, cannot be a member of the same Bohr-Mottelson rotational band as the 277-kev state, since they have different parity.

$Io^{230}$

A gamma ray of 184 kev was observed in the $Io^{230}$ gamma spectrum and in coincidence with alpha particles, L x-rays, and the 68-kev gamma ray.

The gamma ray represents the transition from the 253-kev to the 68-kev state. By analogy with other nuclei in this region, the 253-kev state probably has a spin of 1-.

L x-rays were also observed in coincidence with the 253-kev gamma ray. This indicates that other states are being populated besides the usual 0+, 2+, 4+ rotational band and 1- state. This is similar to what was found in $U^{232}$ decay. *

$Po^{208, 209}$

A gamma ray of 260-kev (0.3%) was found in coincidence with $Po^{209}$ alpha particles. A gamma ray of 910 kev was found in coincidence with K x-rays of $Po^{209}$. The abundance of the coincidences is such that nearly all $Po^{209}$ K-capture events pass through the 910-kev state. The 910-kev gamma ray is 0.4% of the $Po^{209}$ alpha disintegrations. The $Po^{209}$ K x-rays are 0.57% of the $Po^{209}$ alpha disintegrations. K x-rays of some other nuclide, probably $Po^{208}$, were observed in an abundance of 0.002% of the $Po^{208}$ alpha activity. A gamma ray of 290 kev and one or more gamma rays of ~600 kev were observed in coincidence with K x-rays. These gamma rays do not belong to $Po^{209}$ and may belong to $Po^{208}$. Their respective abundances are 0.002% and 0.004% of the $Po^{208}$ alpha particles.

## CONVERSION ELECTRON SPECTRA IN THE HEAVY-ELEMENT REGION

Warren G. Smith and Jack M. Hollander

Spectroscopic studies of the low-energy conversion electron spectra in the heavy-element region are being carried out with two high-resolution photographic recording 180° spectrometers of the permanent-magnet type. Energy calibration has been done with ThB, $I^{131}$, and $Am^{241}$. With fine wire sources of $I^{131}$, resolution of 0.05% has been obtained, but for the samples of $Cm^{242}$, $Am^{241}$, and $Am^{243}$ thus far examined, resolution has not been better than ~0.1%. The actinide element sources are prepared by precipitation

---

*F. Asaro and I. Perlman, "Decay Properties of $U^{232}$," (to be published in Phys. Rev.)

on the (pt wire) cathode of an electrolyte cell as the $M(OH)_3$.

A very brief summary of our results on $Cm^{242}$ and $Am^{241}$ is as follows:

$Cm^{242}$

The energy of the E2 transition between the first excited state and ground state of $Pu^{238}$ has been determined to be 44.11 ± 0.04 kev, from measurement of seven conversion lines. We have also observed the internal conversion coefficient ratios $L_{II}/L_{III} = M_{II}/M_{III} \sim\sim N_{II}/N_{III} = 1.2$, in good agreement with the theoretical value of 1.2 calculated for the $L_{II}/L_{III}$ ratio.[1,2]

$Am^{241}$

Forty conversion lines have been observed in the energy range from 20 to 80 kev that can be assigned to known gamma-ray transitions following the alpha decay of $Am^{241}$. Using for internal standards the energies of two of those gamma rays--59.57 and 33.20 kev as measured recently by Day[3] with a crystal diffraction spectrometer--we obtain values for the other transitions of 26.34, 43.44, 55.54, and 98.99 kev. Day has also determined the first two of these as 26.36 and 43.46 kev.

The 59.57-kev transition is thought to be of multipolarity E1, but previous work on the L conversion electron spectrum, though not resolving the $L_I$ and $L_{II}$ lines, has indicated a discrepancy with the theoretically predicted $L_I/L_{II}/L_{III}$ ratio for this energy and atomic number. Jaffe, Passell, Browne, and Perlman[4] have given for the ratio $L_I + L_{II}/L_{III}$ a value of 4.6, and Wolfson[5] has measured this same ratio as 6.4. Theoretical calculations by Gellman, Griffith, and Stanley[1] and Rose[2] give $L_I = L_{II} = L_{III}$ or $L_I + L_{II}/L_{III} = 2$. We have been able to resolve all the L conversion lines and also the M conversion lines of this transition, and obtain the values $L_I/L_{II}/L_{III} = 1.5/3.1/1.0$ and $M_I/M_{II}/M_{III} = 2.1/3.8/1.0$. (Within our experimental error--as yet unevaluated-- in making these relative intensity determinations, the L ratios and M ratios can probably be considered indentical). Our value of $L_I + L_{II}/L_{III}$ is 4.6, in agreement with Jaffe et al.[4], but still in disagreement with theory.

Work is presently being carried on with $Am^{243}$ in the hope of obtaining similar data for that isotope.

---

[1] [2] Gellman, Griffith, and Stanley, Phys. Rev. 85, 944 (1952).
[2] M. E. Rose et al., privately circulated tables.
[3] P. P. Day, Phys. Rev. 97, 689 (1955).
[4] Jaffe, Passell, Browne, and Perlman, Phys. Rev. 97, 142 (1955).
[5] J. Wolfson, private communication to I. Perlman.

Seaborg

## A STUDY OF ALPHA SYSTEMATICS THROUGH THE GAMOW RELATIONSHIP

Charles Gallagher, Jr., and John Rasmussen

Alpha-decay energies have been correlated with alpha half lives according to a generalized Gamow relationship, $\log \alpha_{t_{1/2}} = AE^{-1/2} + B$, where A and B are assumed smoothly varying functions of Z and of Z and R, respectively. Linear relationships have been found along isotopic lines for even-even alpha emitters plotted in this manner ($\log \alpha_{t_{1/2}}$ against $E_{\alpha}^{-1/2}$).

Interpolation between every two consecutive lines yielded an isotopic line for odd-Z elements. With the slopes (A) and intercepts (B) thus obtained, departure factors have been calculated for all observed energy states to which even-odd, odd-odd, and odd-even alpha-emitting nuclides above 128 neutrons decay.

No departure factors have been calculated for nuclides below 128 neutrons, because irregularities prevail in this region owing to the closing of the 126-neutron and 82-proton shells.

## CONVERSION LINES FROM CURIUM-243 ALPHA DECAY

James F. Schooley and John Rasmussen

During the last quarter of 1954, the electron spectra of several nuclides were investigated; for these studies the double-focusing nuclear spectrometer (beta-ray spectrometer No. 1) was used. The following experimental facts were indicated by the data obtained in these investigations:

1. $Zr^{86}$ (sample obtained from Mitchell G. Florence). K- and L-electron lines corresponding to a transition of 243 ± 2 kev are present with relative intensities of 8.47/1. Only this part of the spectrum was investigated.

2. $Zr^{88}$ (sample obtained from Earl K. Hyde). K- and L-electron lines corresponding to a transition of 387 ± 2 kev are present with relative intensities of 8.39/1. KLL and KL(M, N) Auger electrons are present with relative intensities of 3.61/1. Only these parts of the spectrum were investigated.

3. $Cm^{243}$ (sample obtained from Frank Asaro). K-electron lines corresponding to transitions of 211 ± 2, 228 ± 2, and 278 ± 2 kev are present with relative intensities of 1/2.77/1.48. Limits on the K/L ratio for these three photons are $K/L \geq 1.6$, $\geq 6.4$, $\geq 6.6$. L-lines ascribed to $Cm^{243}$, corresponding to a transition of 46.2 ± 1 kev, are present with relative intensities of $L_I + L_{II} = 2.8$, $L_{III} = 1$.

4. The transmission of the BRS I in these investigations is approximately 0.02 percent. This calculation is based on the counts at the highest point of the peak (minus background) vs. the source activity (computed from other experimental data).

Seaborg

## ALPHA DECAY OF SPHEROIDAL NUCLEI

John Rasmussen and Ben Segall*

The inward numerical integrations of the coupled alpha-decay wave equations[1] in prolate spheroidal coordinates have now been completed for all possible choices of phases for $Cm^{242}$ and for $Th^{228}$. Other evidence leads us to prefer a particular phase choice for each nucleus.

The probability distributions at the spheroidal nuclear surface are strikingly different for $Cm^{242}$ and $Th^{228}$. In $Cm^{242}$, the highest alpha-probability regions on the nuclear surface are at intermediate angles, with nearly zero probabilities at poles and equator. In $Th^{228}$, the highest alpha probability on the surface is in the vicinity of the poles, with nearly zero probability at the equator.

A qualitative theoretical interpretation is that the alpha-probability function on the nuclear surface is simply a measure of the concentration of the lightly bound neutron and proton pairs. One may presume that, between thorium and curium, the proton orbitals occupying the ends of the prolate spheroidal well have been filled and orbitals concentrated at intermediate angles have begun filling.

The initial phase of this study is considered complete, and the results are being prepared for publication.

## THE FAST-COINCIDENCE COUNTING APPARATUS

Donald Strominger and John Rasmussen

The fast-coincidence apparatus previously described by Rasmussen and Kalkstein[2] has been modified. A standard UCRL unit, the "Pulse Shaper and Timing Pulse Generator," has been incorporated into the equipment. This instrument shapes pulses to give them the proper characteristics needed to use the multichannel differential pulse analyzers. This instrument also has provisions for a triple coincidence. This feature enables us to use slow triple-coincidence selection with the pulse from the fast coincidence circuit, the pulse from the single channel analyzer, and the signal pulse itself.

Another change was the replacement of 1N56 diodes with G7A diodes in several critical places in the fast-coincidence circuit. G7A diodes have better high-frequency characteristics than 1N56 diodes, and preliminary experiments do indicate considerable improvement.

---

*Now with Light Production Studies Group, General Electric Research Laboratories, Schenectady, New York.

[1] See previous Quarterly Reports and J. O. Rasmussen, Jr., Theory of Alpha Decay of Spheroidal Nuclei, University of California Radiation Laboratory Report No. UCRL-2431.

[2] J. O. Rasmussen and M. Kalkstein, in Chemistry Division Quarterly Report for Dec. 1953-Feb. 1954, University of California Radiation Laboratory Report No. UCRL-2531.

To test the modified equipment, a delay curve of the alpha-gamma coincidences in the alpha decay of $Cm^{243}$ was made. Graham and Bell[1] measured, using $Np^{239}$, the lifetime of a metastable state 276 kev above the ground state in $Pu^{239}$. They measured the half-life of this state to be $1.1 \times 10^{-9}$ second from the beta decay of $Np^{239}$.

This same level is highly populated in the alpha decay of $Cm^{243}$. A stilbene crystal was used to detect alpha particles, and a sodium iodide crystal was used to detect gamma transitions in coincidence with the alpha particles. The relative intensity of the 276-kev gamma transition in coincidence with alpha particles was studied as a function of delay of both gamma-ray and alpha-particle pulses.

The limiting slope of the delay curve for an instantaneous transition gives an apparent half-life of $8 \times 10^{-10}$ second. Delay-curve integrations yield the result that the combination of the $1.1 \times 10^{-9}$-second half life with the limiting slope will result in a new delay curve with a half life of $1.4 \times 10^{-9}$ second. The experimental slope yielded a half life of $1.5 \times 10^{-9}$ second, in good agreement with the theory. Thus, our results confirm the lifetime measurement of Graham and Bell.

Experiments are now in progress on $Cf^{249}$. Some work was previously reported on this isotope.[2]

## MASS SPECTROMETER APPEARANCE POTENTIALS OF IONS IN DIISOPROPYL ETHER

Herbert X. DiGrazia and Amos S. Newton

The mass-spectrometer appearance potentials of several ions found by the bombardment of diisopropyl ether with electrons have been measured.

| Mass | Ion | Appearance Potential (electron volts) |
|---|---|---|
| 87 | $C_3H_7OCHCH_3^+$ | 9.31 ± 0.02 |
| 59 | $C_3H_7O^+$ | 11.72 ± 0.07 |
| 45 | $CH_3CHOH+$ | 11.03 ± 0.07 |

Mass 45, the largest peak in the mass spectrum of isopropyl ether, must arise from a rearrangement. A postulated mechanism for its formation is as follows:

---

[1] Graham and Bell, Phys. Rev. 83, 222 (1951).

[2] D. Strominger, C. Gallagher, and J. O. Rasmussen, Chemistry Division Quarterly Report for Sept.-Nov. 1954, University of California Radiation Laboratory Report No. UCRL-2841.

Seaborg

$$C_3H_7\text{-}O\text{-}C_3H_7 \xrightarrow{e^-} C_3H_7\text{-}O\text{-}C_3H_7^+ \longrightarrow C_3H_7\text{-}OH^+ + C_3H_6,$$

$$C_3H_7OH^+ \longrightarrow CH_3CHOH^+ + CH_3.$$

The parent mass of diisopropyl ether is Mass 102, but almost no parent ions are formed. Therefore Mass 87, in which one methyl group is lost, is the largest ion formed with reasonable yield.

Mass 59 corresponds to the loss of an isopropyl radical. It is interesting that this has a higher energy requirement than the loss of a propene molecule with a rearrangement of the ion to the isopropyl alcohol molecule ion, which spontaneously dissociates to Mass 45. Isopropyl alcohol has almost no parent peak in its mass spectrum.

These measurements were made with a Consolidated Engineering Corporation mass spectrometer Model 21-103. All peaks were scanned at 1,000 volts accelerating potential and a repeller voltage of about 1 volt. Benzene, krypton, and argon standards were used. The extrapolation to zero was made by the method of Lossing, Ingold, and Henderson,[1] in which the voltage difference between the unknown and standard is plotted against the ion current at percentages of the 50-volt ion current. The appearance potential of Mass 78 in benzene was taken as 9.43 electron volts from the work of Hoing,[2] and from spectroscopic values of krypton and argon of 14.01 and 15.76 electron volts, respectively used. The observed difference between krypton and argon was 1.72 ± 0.02 volts, compared with 1.75 electron volts from the spectroscopic values.

## EQUILIBRIA OF RARE EARTH FLUORIDES

William P. Bryan

A previous quarterly report* has indicated reasons for studying the equilibrium pressures of certain pairs of tri- and tetrafluorides in the rare earth series. The equilibria selected for study are

$$CeF_4(s) = CeF_3(s) + 1/2\ F_2(g) \qquad (1)$$

$$TbF_4(s) = TbF_3(s) + 1/2\ F_2(g) \qquad (2)$$

It is proposed to measure the entropy changes for these reactions by obtaining the temperature coefficients of the free-energy changes of the reactions. In order to do this, one must measure the equilibrium constants or equilibrium pressures of the reactions at various temperatures.

---

[1] F. P. Lossing, K. U. Ingold, and I. H. S. Henderson, J. Chem. Phys. 22, 1489 (1954).

[2] R. E. Honig, J. Chem. Phys. 16, 105 (1948).

*Chemistry Division Quarterly Report, June-August 1954, University of California Radiation Laboratory Report No. UCRL-2709.

The previous report also outlined an effusion method for obtaining values of $P_{F_2}$, the equilibrium pressure. Work was continued on this method. Briefly stated, the method involves hanging an effusion cell made from nickel foil onto a quartz-fibre cantilever balance by means of a fine copper wire. The cell is charged with the rare earth tetrafluoride. The balance and cell are kept under high vacuum. At a temperature at which the equilibrium pressure becomes appreciable, $F_2$ starts to effuse out of the cell, and the cell loses weight. This loss in weight can be measured by watching the movement of a pointer on the cantilever balance through a cathetometer. Assuming equilibrium inside the effusion cell, one can calculate the equilibrium pressure of $F_2$ by means of the Knudsen equation

$$P_{F_2} = \frac{N\sqrt{2\pi MRT}}{at} \qquad (3)$$

where N = number of moles of gas of molecular weight M effusing through an orifice of area a ($cm^2$) in time t (sec).

After the apparatus had been constructed, two difficulties were encountered. The first of these involved the drifting of the pointer over a period of time. Some slight modifications of the apparatus and thorough clamping of the jack on which the balance case was mounted and of the balance case itself finally resulted in a completely stable pointer.

The other difficulty involved vibrations of the sensitive pointer and could be traced to two sources. The first of these was the vibrations inherent in Building 4. A number of schemes, none of them completely successful, was tried in order to eliminate these vibrations. The move to Building 70 will probably eliminate this trouble, although the effusion apparatus has not yet been set up in the new building. Another source of pointer vibrations was bumping of the reflux liquids used to keep the cell at constant temperature. This method of temperature control had to be abandoned, since no scheme could be devised to quiet the pointer sufficiently and yet retain a refluxing liquid in the apparatus.

It was next decided to heat the glass tube containing the effusion cell by means of a metal block heater. A metal block heater was made which was constant to about ±5° C. Such a device would be satisfactory for rough measurements but not for accurate measurements. If the effusion work is continued, it will probably be necessary to make a heater block with automatic temperature control. At present, it seems doubtful if such a device will work above about 350° C.

The effusion method will give accurate results only when the mean free path of the gas molecules within the cell is large compared to the diameter of the orifice. Thus only low pressures ($\sim 10^{-3}$ mm) can be measured using the effusion technique. Accordingly, a new experimental method was developed in order to measure $P_{F_2}$ at higher temperatures and pressures. If both experimental methods turn out to be satisfactory they will serve to check each other.

The new experimental method is a very direct one for measuring $P_{F_2}$. The technique is to suspend a pan with a mixture of tri- and tetrafluorides from a nickel helix balance in an atmosphere with a certain partial pressure

of fluorine, and then to vary the temperature until the pan neither gains nor loses weight.

A fluorine line was constructed for such experiments. The line was nearly all nickel with a little copper, and with brass and bronze fittings. Permatex-2 gasket cement was used as luting for the fitting threads. A long nickel chamber made from a 1-inch-diameter nickel tube was used to house the nickel helix balance, which was made from 3-mil nickel wire and had a sensitivity of roughly 1 mm/mg.

Only $F_2$ at a pressure of about 40 psi was used, and it was obtained by bleeding from a cylinder containing a maximum of 400 psi of $F_2$. The fluorine pressure could be read on brass Bourdon gauges. Provision was made so that the system could be evacuated or swept with argon. It is possible to make a synthetic mixture of $F_2$ and A in the secondary cylinder and then pass this gas into the evacuated line.

In order to obtain $P_{F_2}$ accurately it is necessary to analyze the gas in the line. The method adopted here is to pass the gaseous mixture (A and $F_2$) through nickel traps filled with KBr and heated to 150° C. Under these conditions, all the $F_2$ is quantitatively converted to $Br_2$. The $Br_2$ can then be passed through potassium iodide solution and the resulting $I_3^-$ produced can be analyzed by standard procedures. This analytical method has not yet been tested experimentally.

Another feature of interest in the apparatus is the windows used to observe the motion of the nickel helix. These are made of transparent fluoroethylene and are sealed in place with nickel and brass fittings. They retain complete transparency when the nickel chamber contains $F_2$ at 1 atmosphere pressure.

When the balance is loaded with about 100 mg of rare earth tetrafluoride, it is estimated that it is easily possible to tell when about 1 percent of the tetrafluoride has been converted to trifluoride. Thus if the balance is loaded with tetrafluoride and slowly heated in an atmosphere containing a given pressure of fluorine, the equilibrium temperature for this pressure can be readily obtained. Temperatures are measured with a thermocouple enclosed in a well in the balance chamber.

A few preliminary measurements have been made with the apparatus. $CeF_3$ was found to take up $F_2$ (~1 atm pressure) at from ~100 to 200° C. An x-ray analysis confirmed that the resulting product was $CeF_4$. When this $CeF_4$ was heated in the balance in an atmosphere of argon, anomalous results were obtained. At ~520° C to 660° C the sample gained weight. This gain is hard to explain, and more work is necessary to clarify the situation.

A small sample of $Tb_4O_7$ was available, although not enough for accurate work with the balance. Upon being heated in a $F_2$ atmosphere at 240° the oxide was converted to a fluoride (presumably $TbF_4$).

At present, samples of $TbF_4$ and $CeF_4$ are being heated in high vacuum at temperatures of ~450° C to see if the trifluorides can be produced. If they cannot be formed at such temperatures it may be difficult to use the helix balance, since the nickel wire may disintegrate when exposed to $F_2$ at temperatures much above 450°. Further work will clarify this situation.
Seaborg

## LIGHT RHENIUM ISOTOPES

Michael Sweeney and John Rasmussen

Stacked-foil excitation-function experiments with 48-Mev alpha particles on tantalum were carried out. Decay of Geiger counter activity was followed for the foils with no chemical separations. Predominant features of the excitation function at energies of 35 Mev and above are the peaking of the yield of a ~64-hour activity (presumably $Re^{182}$) at about 38 Mev, and the substantial amount of ~18-hour activity with apparent threshold near 38 Mev and rising yield at 47.5 Mev. The ~18-hour activity we tentatively assign to hitherto unreported $Re^{181}$, on the basis of the similarity between its excitation function and that expected for (α, 4n).

## SEARCH FOR AMMONIATED ELECTRONS IN LIQUID AMMONIA BOMBARDED WITH ELECTRONS

Amos S. Newton

For some time there has been a controversy on whether or not slow electrons formed in the irradiation of water or ammonia would be solvated.[1] A search for such solvated electrons in liquid ammonia was made by Roberts and Allen,[2] who measured the electrical conductivity of ammonia during and after irradiation with negative results. Linschitz[1] has looked for a blue color in water after irradiation using a pulsed beam, a monochromatic light source, and a photocell detector, again with negative results.

From the half width of the electron resonance line of sodium solutions in liquid ammonia in nuclear magnetic resonance apparatus, it is estimated that the mean lifetime of the electron in the solvated state is $10^{-5}$ second or less in sodium solutions. Therefore, an apparatus must be capable of seeing an absorption a few microseconds after bombardment.

An apparatus was made in which ammonia was bombarded with 2.5-Mev electrons from a microwave accelerator. The accelerator gave a pulse of 2-microsecond duration with about $2 \times 10^{12}$ electrons per pulse. If 30 electron volts yielded one secondary electron and all were solvated, this would yield about $1.5 \times 10^{17}$ solvated electrons in a volume of about 10 ml, or a concentration of about $2 \times 10^{-5}$ M solvated electrons at the end of the pulse. Losses of fast electrons by scattering and losses of secondaries by ion recombination would reduce this concentration considerably.

The apparatus is shown diagramatically in Fig. 1.

---

[1] "Basic Mechanisms in Radiobiology," J. G. Magee, M. D. Kamen, and R. L. Platzman, editors, National Academy of Science, National Research Council, Publication 305, Washington, D. C., 1953, p. 31-40.

[2] R. Roberts and A. O. Allen, J. Am. Chem. Soc. 75, 1256 (1953).

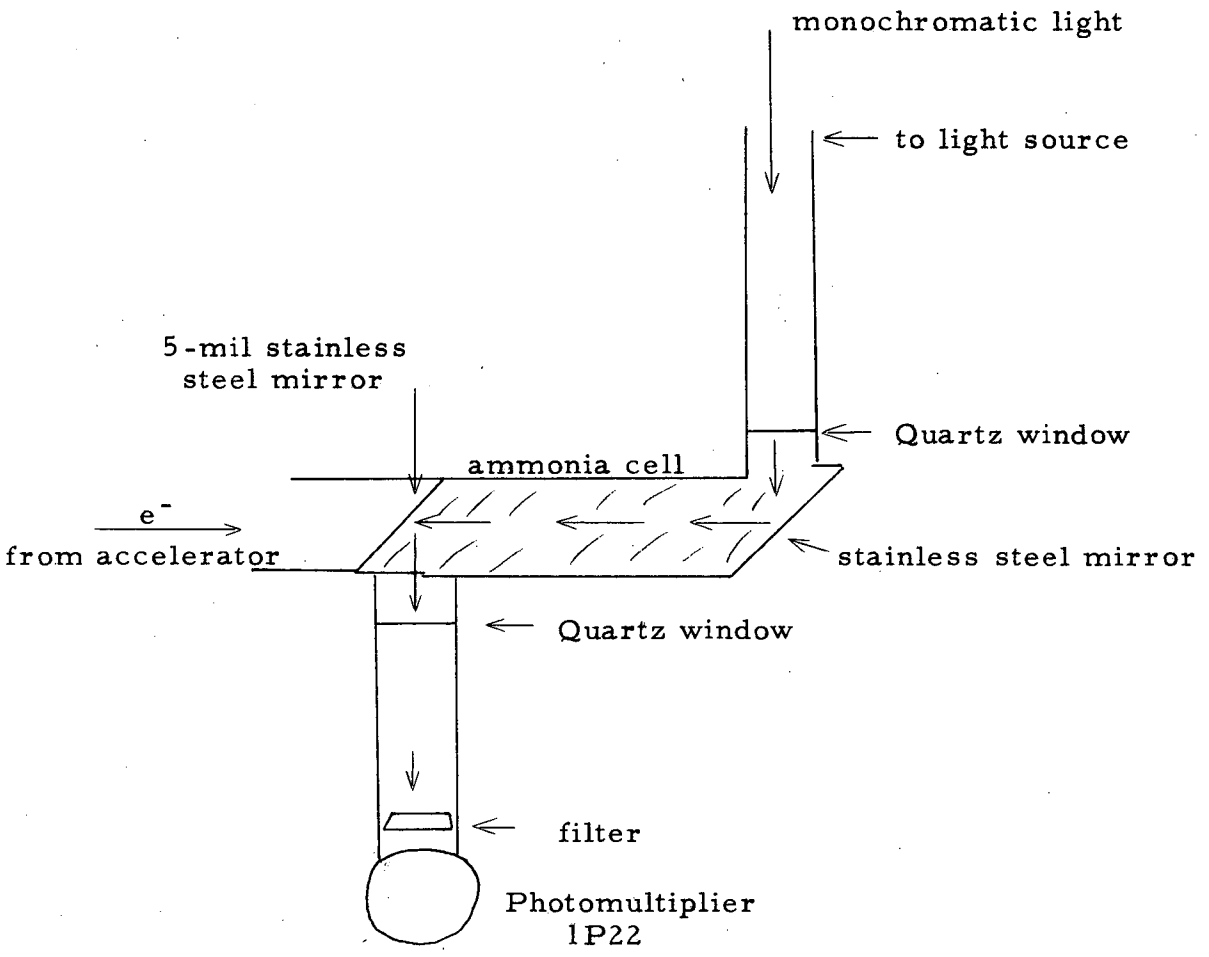


Fig. 1. Apparatus for electron bombardment of ammonia.

The monochromatic light source was a Beckman Model DU spectrophotometer with the cell carriage removed and a tube attached containing 2 achromatic lenses for rendering a parallel light beam to the ammonia cell. The light then passed through a quartz window, into the cell, reflected down the tube and out the other side by the two 45° mirrors, and was focused on the IP22 photomultiplier element. The entire cell was cooled to about -70° C with dry ice packed around it.

Since the absorption of sodium solutions of liquid ammonia increase with wave length and the response of the photomultiplier decreases with wave length, the region 6,000 to 7,000 A was searched. The output of the photomultiplier was fed into either a Tektronix Model 513D or Model 512 oscilloscope and a search was made for a change in output in the few microseconds immediately following bombardment. Because of a fluorescence in the ammonia, a filter cutting off all light below 5,800 A was placed immediately before the photomultiplier.

During bombardment there was a large increase in photomultiplier output due to x-rays. This output during bombardment was not changed by cutting out all light to the photomultiplier.

No change in photomultiplier response over about 0.5 microsecond after the bombardment was observed, i.e., there was no absorption within our detectable limits of about 5 percent that had a lifetime greater than about 0.5 microsecond.

This does not prove that solvated electrons are not formed, since a calculation using values of the molar extinction coefficient of sodium solutions in liquid ammonia as found by Gibson and Argo[3] and Jolly,[4] shows that at 7,000 A a concentration of $4 \times 10^{-5}$ M electrons would only give 1 percent absorption. Therefore, the experiment lacked at least a factor of 10 or 100 in sensitivity for obtaining a definite result. An increase in sensitivity by such a factor could be found in (1) increasing the signal-to-noise ratio in the photomultiplier and oscilloscope circuits, (2) increasing the electron beam, or (3) the use of a fast infrared detector at 15,000 A, where the molar extinction coefficient is about 40,800 compared to 855 at 7,000 A.

Since none of these possibilities was feasible at present the experiment was temporarily abandoned.

## ALPHA-TRACK COUNTER

Archie B. Treadwell, Herman P. Robinson, and G. Donald Paxson

Favorable progress is being made on an instrument to automatically count and record the distribution of 3.5- to 9-Mev alpha tracks in a photographic emulsion. The instrument is designed to handle the 5-by-22-cm glass plates

---

[3] G. E. Gibson and W. L. Argo, Phys. Rev. 7, 33 (1916); J. Am. Chem. Soc. 40, 1327 (1918).

[4] W. L. Jolly, Absorption Spectroscopy in Liquid Ammonia, University of California Radiation Laboratory Report No. UCRL-2008, Oct. 1952, p. 14.

from the alpha spectrometer. By use of a modulated dark-field illumination and a photomultiplier, the tracks are caused to produce an alternating current signal, delineating them from the background of random grains and dust particles which produce only direct current signals. Electronic components will automatically treat the ac signals from the tracks and plot a graph of absolute track density as a function of distance from the end of the plate. Despite the extremely small size of the tracks, 40 by 0.4 microns, a satisfactory signal of 30 millivolts with a 5-to-1 signal-to-noise ratio has been achieved. It is to be noted that the instrument is of use only in counting tracks that are all parallel to one another.

## MASS SPECTROSCOPY: VACUUM VALVES

Frederick L. Reynolds

During the past several years, a number of ideas have been presented in the instrument literature pertaining to vacuum valves suitable for use with mass spectrometers.[1-6] Most of these valves employ rubber O-ring seals, or employ complicated differential pumping methods. The need for a simple, positive shutoff valve, having no leak rate and containing no organic materials, has been apparent in this field for some time.

A valve meeting these requirements has been made and tested. Its primary function is to isolate the trap and diffusion-pump system from the trajectory system during sample changes.

The valve consists of a copper block milled as shown in Fig. 2. The top circular groove is filled with indium metal and acts as the valve seat. The cap, also made of copper, is coated on the sides with indium metal. The lower milled groove contains a spiral-wound nichrome heater of proper resistance to operate off a 110 volt ac line. To open the valve requires about two minutes to melt the indium, and the valve cap can be raised by a suitable mechanical lever operated through a sealed sylphon. With the closing operation the procedure is reversed. The valve has to be operated in the vertical position, and in this application is not opened against atmospheric pressure.

The operation has been checked using a helium leak detector, a positive vacuum seal resulting. The vapor pressure of indium at its melting point is very low.

---

[1] Decker, All Glass Valves for Use in Obtaining Ultra High Vacuum, J. App. Physics 25, 1441 (1954).
[2] Fultz, A Metal Vacuum Lock for a Mass Spectrometer, Y-990.
[3] Stevens, Vacuum Lock for a Mass Spectrometer, AECU-1996.
[4] Alpert, Vacuum Valve, Rev. Sci. Instr. 22, 536 (1951).
[5] Cameron, A Compact High Vacuum Valve, K-1020.
[6] Fox, A Large-Diameter Reciprocating Action Vacuum Valve, MLM-850.

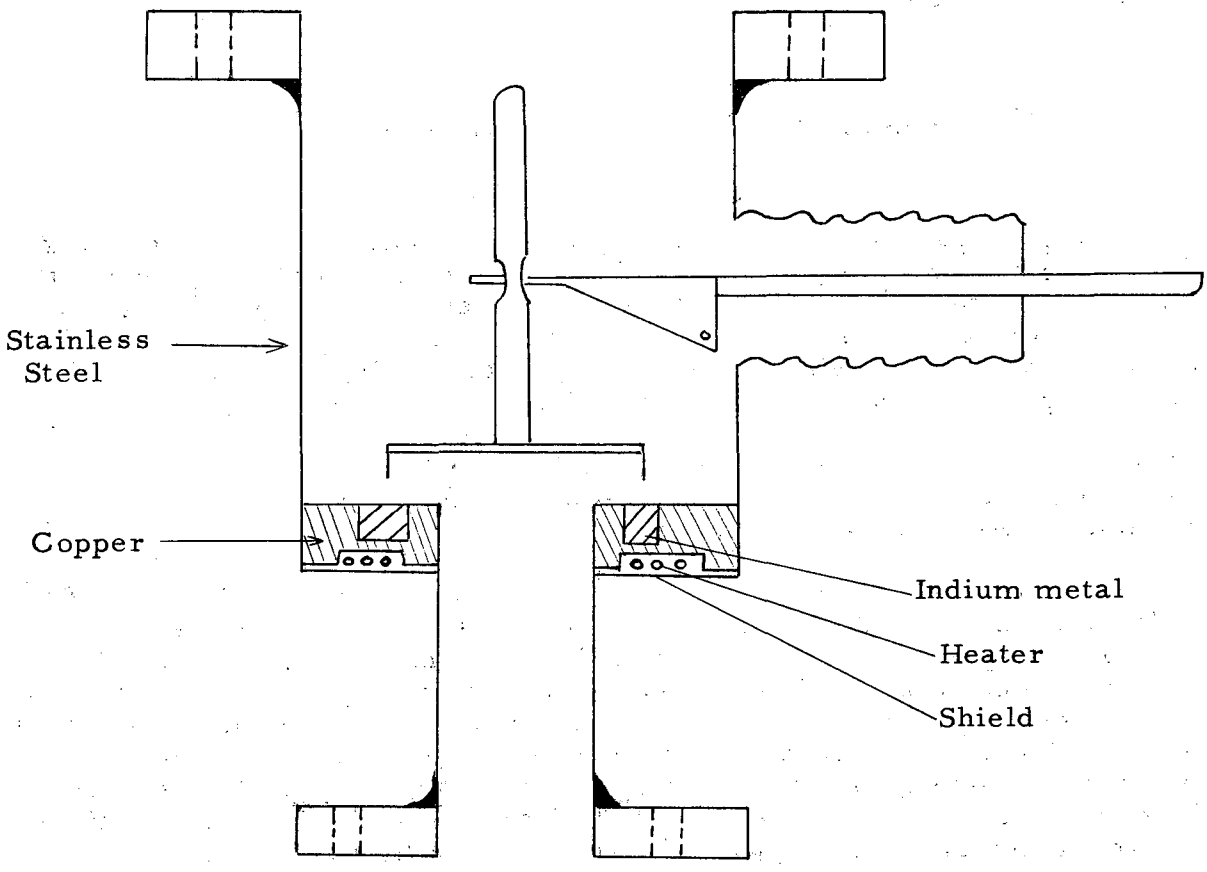


Fig. 2. Shutoff valve for mass spectroscope.

# MASS SPECTROSCOPY: ION SOURCES

Frederick L. Reynolds and Russell G. Herron

Point field-emission positive-ion-source studies[1] were continued. Electron-microscope photographs of tungsten points were taken in the University of California electron microscope (RCA Model B). Calculations indicated the radius of curvature of the point at the tip was $2.15 \times 10^{-5}$ centimeters. This value is of the same magnitude as that reported by other workers[2] in point emission studies.

Experiments concerning the transfer rate of solid samples as ions from the point were commenced. $Cm^{242}$ was deposited in the region of the point by physical contact. Preliminary qualitative results indicate $Cm^{242}$ is transferred from point to collector under favorable conditions of voltage and temperature. Further experiments to determine the nature of the voltage-thermal relations will be done using $Cm^{242}$. It is intended to use the findings in the evaluation of the point field-emission positive-ion source as a practical source for mass spectrometers. Experiments to date indicate that at 1,100° Kelvin curium ions are removed from the point by high electrostatic fields, and that in the absence of high fields, no transfer of ions or neutral atoms of curium occurs at the above temperature.

---

[1] Chemistry Division Quarterly Report for September-December 1954, University of California Radiation Laboratory Report No. UCRL-2841.

[2] E. W. Muller, Phys. Z. 37, 838 (1936).

# CHEMICAL ENGINEERING (PROCESS CHEMISTRY)

## NOTES ON WORK IN PROGRESS

### The Effect of Fluid Properties on the Mass Transfer Rate in the Gas Phase

Robert J. Fallat and Charles R. Wilke

The work of Dr. Edward Lynch concerning correlations between heights of transfer units ($HTU_G$) and Reynolds number is being extended to higher pressures in order to clarify the conclusions reached from the previous work. A high-pressure apparatus has been designed and is now being built. Also, since vapor pressure of naphthalene is a critical property involved in the work, a unit for measuring vapor pressure at various temperatures has been set up and data are now being collected.

### Thermal Conductivity of Gases at High Temperatures

Henry Cheung and Charles R. Wilke

A study of Dr. A. L. Rothman's data and experimental technique has been completed. Calibration of the several capillary manometers to be used for mixing gases is in progress.

### Gas-Phase Mass Transfer Studies

Loren J. Hov and Charles R. Wilke

During the preceding period a new sampling device was completed, and psychrometric studies are now in progress covering the range of film pressure factors from 1.0 to 0.1. At present, no simple correlation between psychrometric ratio and film-pressure factors is obtainable from these data.

### Stability of Perforated Plate Trays

Robert S. Brown, Donald N. Hanson, and Charles R. Wilke

The design of the apparatus for this study has been completed. The apparatus is now being manufactured.

### Vacuum Flow through Annular Sections

Walter Dong and Donald N. Hanson

Calculations are being made on the velocity distribution of the gas near the surface of the duct in the slip-flow region. Additional experimental measurements are planned to check present data.

## Correlation of Limiting Current Density at Horizontal Electrodes Under Free Convection Conditions

Eugene J. Fenech and Charles W. Tobias

Equipment has been designed, built, and set up in Room 158, Building 70. Experimental procedure and conditions have been decided upon and work is about to commence.

## Liquid-Liquid Extraction and Agitation

R. H. Houston and Theodore Vermeulen

The minimum intensity of mixing that is necessary to produce bulk homogeneity has been found in previous work to give a very economical condition of mixing. A method of predicting this homogeneity, or "bulk mixing index," has been derived from theoretical grounds and is now being tested experimentally.

# GENERAL CHEMISTRY

W. M. Latimer, Director

## METALS AND HIGH-TEMPERATURE THERMODYNAMICS

Leo Brewer, Richard Brewer, John Engelke, William Hicks, James Kane, Oscar Krikorian, Geoffrey James, and Lewis Roberts

### Vaporization and Condensation Coefficients of Molecular Beams

A mass spectroscopic examination of phosphorus and arsenic vapor has been done in cooperation with Professor Reynolds. It is believed that the vaporization mechanisms have been largely clarified, and the final results of the work are being written up for publication.

### Oxide Reaction Studies

Oxygen exchange studies of $UO_2$-$ThO_2$ solid solutions have been carried out. $ThO_2$ exchanges completely at 800°C. The oxygen taken up by uranium in the solid solutions at lower temperatures does not exchange completely with the lattice oxygen.

### Molybdenum Gaseous Oxy-Hydroxy-Halides

The formula $MoO_2OHCl$ has definitely been established for the stable gaseous molecule in the Mo-O-H-Cl system.

### Study of SO and $C_2$ Gases

Further progress has been made toward establishing the ground states and heats of formation, but sufficient accuracy has not yet been obtained.

### Determination of Absolute f values

The main features of the apparatus for obtaining absolute absorption coefficients of high-temperature gases have been designed.

# BASIC CHEMISTRY, INCLUDING METAL CHELATES

John Below, Howard Cady, Robert E. Connick, Laddie Griffith, Armine Paul, and Robert Wood

## Additional Fluoride Complexing Results

The heats and entropies of the reactions

$$Zn^{++} + HF = ZnF^{+} + H^{+},$$

$$Cu^{++} + HF = CuF^{+} + H^{+},$$

$$Hg^{++} + HF = HgF^{+} + H^{+}, \text{ and}$$

$$Ag^{+} + F^{-} = AgF_{(aq)}$$

were determined. Because of the weak complexing, the uncertainties in the heats and entropies are quite high and it is therefore difficult to give much theoretical significance to them. It does appear, however, that the entropies are somewhat more negative than one would expect.

Further studies were made on the fluoride complexing of $Sn^{++}$. The fluoride concentration was determined spectrophotometrically by measuring the displacement of the uranyl fluoride equilibria when stannous ion was added. Although not as accurate as the EMF measurements, the results are in agreement with the EMF determinations. The EMF measurements at high stannous concentrations and low acidities cannot be interpreted. At high acid (>0.5 M) and low stannous concentrations (0.001 - 0.01 M) an equilibrium quotient of about 20 was obtained for the reaction $Sn^{++} + HF = SnF^{+} + H^{+}$ at 25° and $\mu = 0.5$.

## The Spectrophotometric Study of Rapid Reactions: The Kinetics of the Reaction between Ferric Ion and Thiocyanate Ion

The rapid mixing and spectrophotometric recording device previously described have been used to study the reaction between $Fe(ClO_4)_3$ and NaSCN in $HClO_4$–$NaClO_4$ solutions. It has been found to proceed, in the acid range of 0.01 to 0.3 M, by two paths:

$$(1)\quad Fe^{+++}_{Aq} + SCN^{-} \xrightarrow{k_2} Fe(SCN)^{++},$$

and

$$(2)\quad Fe^{+++}_{Aq} + H_2O \underset{}{\overset{K_H}{\rightleftharpoons}} Fe(OH)^{++} + H^{+} \quad \text{(rapid)}$$

and

$$Fe(OH)^{++} + SCN^{-} \xrightarrow{k_2'} [Fe(OH)(SCN)^{+}],$$

$$[Fe(OH)(SCN)^{++}] + H^{+} \longrightarrow Fe(SCN)^{++} + H_2O \quad \text{(rapid)},$$

leading to the rate law:

$$-\frac{d(SCN^-)}{dt} = k_2(Fe^{+3})(SCN^-) + K_2' K_H \frac{(Fe^{+3})(SCN^-)}{(H^+)} .$$

The values of $k_2$, $k_2'$, $\Delta H^{\ddagger}$, $\Delta S^{\ddagger}$, $\Delta H^{\ddagger'}$ and $\Delta S^{\ddagger'}$ are now being calculated from the data. In 0.200 M $HClO_4$ and an ionic strength of 0.4, the effective rate constant $\frac{(k_2 + k_2' K_H)}{[H^+]}$ is $2.3 \pm 0.2 \times 10^2$ $M^{-1}$-$sec^{-1}$.

Radiation-Induced Reactions in Nonaqueous Solutions

The investigation of the rate of disappearance of diphenyl-picrylhydrazyl in chloroform, benzene, toluene, and carbon tetrachloride in the presence of radiation is being extended into the region of x-rays. An attempt is being made to check work done by A. Chapiro (Paris) in this field. Chapiro carried out all radiations in the presence of oxygen. I am carrying out Chapiro's experiments in the absence of oxygen. New equipment is almost complete and quantitative measurement of the quantum yield, Q value, and rate data of uv and x-ray-induced reactions will be made.

Ru Chemistry

$RuO_4$ reacts with excess $H_2O_2$ in acid solution to form a light yellow solution. The spectra show that the solution contains no $RuO_4$. When the yellow solution is evaporated to dryness under vacuum, a black amorphous solid is formed. Most of the solid is soluble in $H_2O$ and ether. Both solutions are dark blue to black in color. An attempt to evaporate the ether layer to dryness caused decomposition of the Ru compound. A dark brown material insoluble in ether was formed. The black $H_2O$ solution turned red-brown upon exposure to air. All changes were irreversible.

The Entropy of the Selenide Ion in Aqueous Solutions

Sodium selenide prepared in liquid ammonia gives a hydrolysis constant for the selenide ion that is greater than 1/2.

Latimer

Information Division
4-7-55 ba